

WAVE EFFECTS OF A FREE SURFACE PIERCING HYDROFOIL

by

Edward C. Kern, Jr.

A.B.
Dartmouth College
(1967)

B.E.
Thayer School of Engineering
Dartmouth College
(1968)

S.M., Naval Architecture and Marine Engineering
Massachusetts Institute of Technology
(1971)

Ocean Engineer
Massachusetts Institute of Technology
(1971)

Submitted in
partial fulfillment
of the requirements for the
Degree of Doctor of Philosophy

at the

MASSACHUSETTS INSTITUTE OF TECHNOLOGY
May 1973

Signature redacted

Signature of Author:

Department of Ocean Engineering
May 18, 1973

Signature redacted

Certified by:

Thesis Supervisor

Signature redacted

Accepted by:

Chairman, Departmental Committee on
Graduate Students



WAVE EFFECTS OF A FREE SURFACE PIERCING HYDROFOIL

by

Edward Clarence Kern, Jr.

Submitted to the Department of Ocean Engineering on May 18, 1973, in partial fulfillment of the requirements for the degree of Doctor of Philosophy.

ABSTRACT

A lifting surface theory is developed for vertically oriented hydrofoils piercing a fluid free surface. The formulation, a singular integral equation, is shown to reduce to known limiting forms for the cases of zero and infinite Froude number. Conditions restricting the mathematical nature of acceptable foil loadings are given for the general case for finite nonzero aspect ratio and Froude number. Two simple foil loadings are numerically investigated, demonstrating the feasibility of a proposed technique for analyzing the dynamics of arbitrarily shaped free surface piercing hydrofoils.

Thesis Supervisor: Professor Jerome H. Milgram
Title: Associate Professor of Naval Architecture

CONTENTS

	<u>Page</u>
Title Page	1
Abstract	2
Contents	3
List of Figures	5
List of Tables	5
Symbols	6
Acknowledgements	8
Introduction	9
I Statement of the Problem	11
II Fundamental Equations	13
III Formulation of the Solution in Terms of a Dipole Sheet	18
IV The Horseshoe Vortex Integral Equation Formulation	25
V The Zero Froude Number ($F \rightarrow \infty$) Limit	28
VI The Infinite Froude Number Limit ($F \rightarrow 0$)	30
VII Lifting Line Theory	33
VIII Permissible Loadings	36
IX Loading Modes	43
X Modification of the Formulation for Numerical Calculations	49
XI Numerical Results	52
XII Conclusions and Future Directions	63
Bibliography	65

	<u>Page</u>
Appendices	
A Transformation from the Dipole to Horseshoe Vortex Formulation	67
B Transformation from Horseshoe Vortex to Newman's and Robinson and Laurmann's Form	69
C The Infinite Froude Number Limit of the Double Integral Term in the Horseshoe Vortex Kernel	71
D Vertical Load Restrictions for Lifting Lines	75
E Free Surface Elevation Discontinuities	77
F Conversion between Forms of the Free Surface Source Potential	79
G Wave Effects of the Horseshoe Vortex Singularity	81
H Listings of Computer Programs Used to Evaluate Distributed Load Downwash Contributions from the Double Integral in the Horseshoe Vortex Kernel Using Loading Transforms	85
I Listings of Computer Programs Used to Evaluate Distributed Load Downwash Contributions from the Zero Froude Number Terms in the Horseshoe Vortex Kernel	99
J List of Computer Programs Used to Evaluate the Downwash of a Point Horseshoe Vortex Singularity	105
Biographical Note	117

LIST OF FIGURES

<u>Figure</u>		<u>Page</u>
1	Dimensional coordinate system	12
2	Nondimensional coordinate system	12
3	Conventions of positive dipole moment, potential jump, vorticity, side force, circulation and pressure jump	23
4	Glauert series mode angle definitions	44
5	Downwash for elliptical spanwise and chordwise loading	54
6	Mean line for elliptical spanwise and chordwise loading	55
7	Downwash for cubic spanwise and elliptical chordwise loading	56
8	Mean line for cubic spanwise and elliptical chordwise loading	57
9	Idealized transverse wave system of a surface piercing hydrofoil	60
10	Downwash variation with depth under a free surface for elliptical spanwise and chordwise loading	62
11	Point horseshoe vortex singularity: downwash versus $(x - x_0)$ for various Froude numbers at fixed $y + y_0 = 1$	82
12	Point horseshoe vortex singularity: downwash versus $(x - x_0)$ for varying $(y + y_0)$ at fixed $F_n = 1$	83

LIST OF TABLES

<u>Table</u>		<u>Page</u>
1	Spanwise loadings and their transforms	45
2	Chordwise loadings and their transforms	47

SYMBOLS

x	coordinate positive upstream
y	coordinate positive downward
z	coordinate positive to port
(x_0, y_0, z_0)	corresponding dummy variables
r	distance from a field point to a singularity in the flow
r'	distance from a field point to an image singularity about the plane at the free surface
C_0	dimensional chord
S_0	dimensional span
g	acceleration of gravity
ρ	the density of water
$AR = S_0/C_0$	Aspect Ratio
U	Free stream velocity in the negative x direction
$\nu = g/U^2$	A parameter of dimension, $1/\text{length}$
$F = gC_0/U^2$	Inverse of the Froude number squared
$F_n = 1/\sqrt{F}$	Froude number
$\Phi = -Ux + \phi$	total velocity potential
ϕ	perturbation potential
ϕ_s	point source potential
ϕ_d	point dipole potential
\vec{V}	total velocity vector
u, v, w	perturbation velocities
$z_{m\ell}$	the dimensionless (fractional chord) foil mean line (surface) distance from the plane $z = 0$
η	the free surface elevation, positive downward

$C_p = \frac{p-p_\infty}{\frac{1}{2}\rho U^2}$	pressure coefficient
$\Gamma(x,y)$	The circulation from one point on the foil's surface to the adjacent point on the opposite surface. This also is equal to the dipole sheet strength at (x,y) .
$\Gamma(y)$	circulation about a lifting line
$\Delta\phi(x,y)$	potential jump across a foil
$\gamma(x,y)$	bound vorticity density (per unit area)
$\Delta p(x,y)$	pressure jump across a foil
ϕ_{S_o}, ϕ_{C_o}	angles associated with the definitions of the Glauert series loadings
Im	The imaginary part of a complex equation
Re	The real part of a complex equation
I	An arbitrary integral's value
γ'	Euler's constant = .5772156649...
$X(x_o)$	Chordwise foil loading
$Y(y_o)$	Spanwise foil loading
\bar{X}	Fourier transform of the chordwise loading
\bar{Y}	Laplace transform of the spanwise loading
\int	An integration where the Cauchy Principal value is to be taken
\int_{-}	An integration whose path is to be taken below a pole into the lower half of the complex plane
\int_{∞}	An integration where the "finite part" is to be taken according to Mangler's "recipe" as set forth in Ashley and Landahl (10) (pp. 130-131)

ACKNOWLEDGEMENTS

The author gratefully acknowledges the continued advice, assistance and guidance of his thesis supervisor, Professor Jerome H. Milgram, during the entire period of the author's graduate study at Massachusetts Institute of Technology. Professor J. N. Newman, who initially proposed this research to the author, never seemed too busy when his advice on some matter was needed. Finally, Dr. K. June Bai's aid has been most helpful. The expert assistance of Diane Wyszomirski in preparing the final manuscript is truly appreciated.

The author was supported during this project partially by the Navy's Surface Effect Ships Project Office contract #2-23560 and partially by grant GK 10846 from the National Science Foundation.

INTRODUCTION

A surface piercing hydrofoil may be any of a variety of winglike bodies moving with constant velocity at a fluid free surface and oriented with part of the wing above and part below the free surface. A partial list of examples includes ship's rudders, streamlined vertical struts used to support horizontal hydrofoils and rigid sidewalls of air cushion vehicles. All of the above are, to some extent, thin bodies which experience large transverse forces when yawed a small angle from straight ahead motion.

Were the fluid free surface eliminated by considering the space above it occupied by fluid and the body's mirror image, the physical situation could be mathematically modeled using techniques of classical subsonic wing theory or slender body theory. Very specifically, the present theory for surface piercing hydrofoils is an extension of lifting surface theory to include the effect of a fluid free surface. As in classical lifting surface theory, the analysis for lifting and thickness effects can be treated independently and only lifting effects are considered herein. It is interesting to note that the corresponding thickness effects in free surface flows have been understood since 1898 when J. H. Michell wrote his famous paper on the wave resistance of a thin ship (20).*

* Numbers in parentheses refer to references listed in the bibliography.

Mathematically, the analysis makes many of the same assumptions as classical lifting surface theory: the body has no thickness and the angle between it and the flow is everywhere small. In addition, the perturbation to the flow by the body must satisfy certain conditions restricting the nature of the waves associated with the flow. These conditions are known collectively as the free surface boundary conditions.

As in lifting surface theory, the ultimate goal of the analysis is to relate the shape of a surface piercing foil to the forces that act upon it when it moves across a free surface. With the present theory the shape of a surface piercing hydrofoil can be obtained directly in terms of the load distribution it is required to achieve. Reversal of the order of solution is a complex but relatively straightforward task, and is often referred to as the inverse problem. The method of the inverse problem in the present theory is simply to superpose solutions to the direct problem in such a way as to generate the desired hydrofoil shape.

Previous known studies of surface piercing hydrofoils have been made by Newman (1), Milgram (2) and Daoud (22). The Newman paper is by far the most comprehensive. Daoud has developed a numerical procedure and has extensively studied lifting surfaces of relatively low aspect ratio.*

* After this final draft was completed, another paper on this subject by Ismail (24) was brought to the attention of the author. It reports on analytic and experimental work on vertical foils. The experiments included cases in which the foil pierced the free surface, but the analytic work addressed itself primarily to foils which are completely below the free surface.

I STATEMENT OF THE PROBLEM

A surface piercing hydrofoil of rectangular planform is assumed to move with constant speed in the positive x direction. The plane $y = 0$, is that of an undisturbed free surface and the positive y direction is taken downward in the direction of gravitational acceleration. The transverse coordinate z is taken positive to port. The surface piercing hydrofoil is situated near the plane, $z = 0$, (because the foil is thin, of small camber and angle of attack) and, establishing the coordinates moving with the foil, the leading edge is taken to be at $x = C_0$ (the chord length), the trailing edge at $x = 0$ and the lower tip at $y = S_0$ (the span). These conventions are shown on Figure 1.

Letting the lengths be nondimensionalized using the chord length, C_0 , and defining the aspect ratio, AR , to be S_0/C_0 , the analysis is simplified by a reduction of the number of parameters. Of particular interest is the parameter, gC_0/U^2 , which is the inverse of the Froude number squared. This parameter, referred to as F , is central to the analysis. Figure 2 shows the nondimensional formulation. For the purposes of simplicity, the dimensionless variables are assigned the same symbol as their nondimensional counterpart. Further use of the dimensional form is anticipated only when developing the lifting line formulation. The free surface height η is measured in the positive y direction.

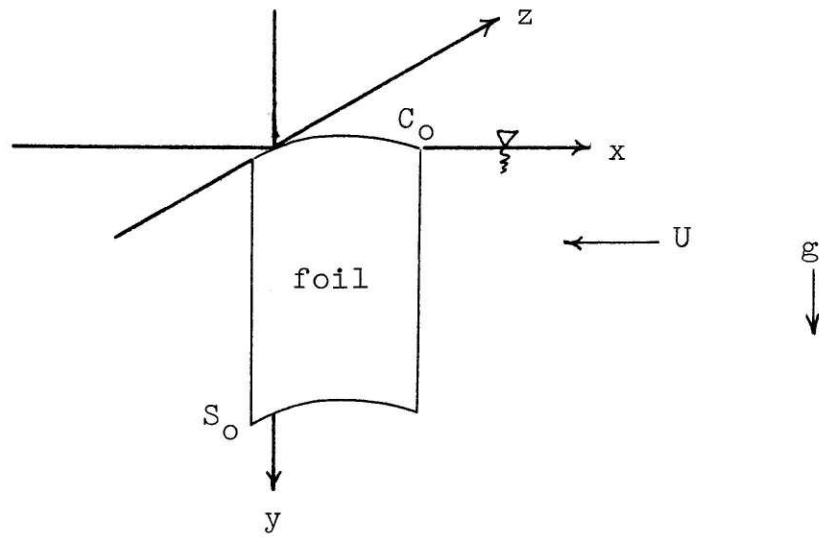


Figure 1 Dimensional coordinate system

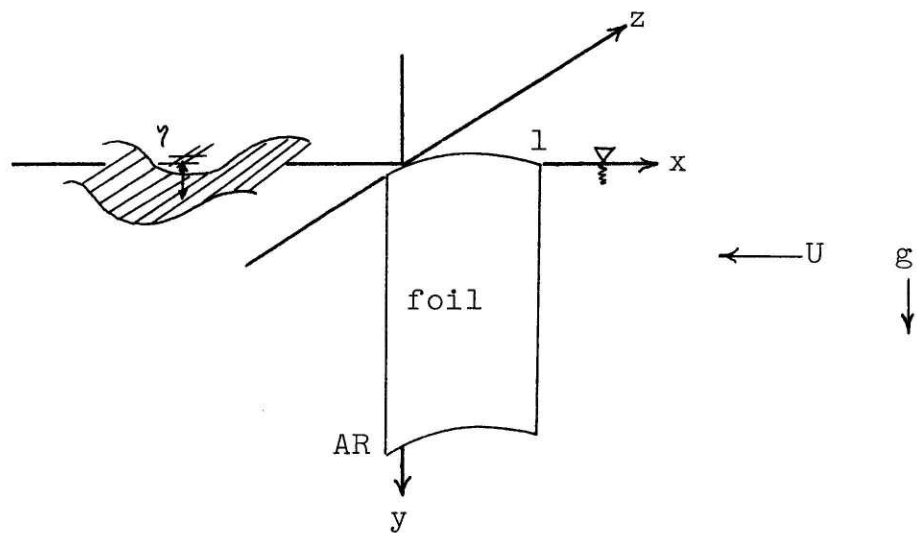


Figure 2 Nondimensional coordinate system

II FUNDAMENTAL EQUATIONS

Both the direct (known loading, unknown shape) and the inverse (unknown loading, known shape) analysis require determination of flow details near the surface piercing foil in terms of other known conditions of the flow at the foil. The inverse analysis specifies that the flow be tangent to the surface of the foil, whereas the direct problem specifies the pressure difference across the foil planform. In both cases other physically motivated restrictive conditions are required of the solution. These are that (i) the flow velocities be finite at the trailing edge (the Kutta condition); (ii) that fluid particles on free surface move with the free surface; (iii) that the pressure at the free surface remain constant; (iv) that any waves generated radiate from the body and decay in amplitude at a rate such that wave energy is conserved. Finally, the flow must satisfy the conservation of mass equation for an inviscid incompressible fluid.

Assuming a velocity potential Φ represents the flow field and that $\vec{V} = \nabla\Phi$, the above conditions can be mathematically formalized for the flow region, $y \geq 0$:

Letting ϕ be a perturbation potential such that $\Phi = -Ux + \phi$, the following conditions are imposed on the solution for ϕ .

(i) The body boundary condition requires that the flow be tangent to the body surface and is written

$$\nabla \Phi \cdot \vec{n} = 0 \quad \text{on } z = z_{ml}(x, y) \quad (2.1.1)$$

where \vec{n} is a unit vector normal to the body surface and z_{ml} is the location of the body surface (here the mean line of the body).

(ii) The Kutta Condition from airfoil theory requires that pressures be continuous across the wing surface at the trailing edge and, in so doing, affords a method of uniquely setting the circulation and lift for the wing. Requiring only that $\nabla \Phi$ be bounded at the trailing edge suffices to satisfy this condition.

(iii) The Kinematic boundary condition on the free surface requires that a fluid particle on the free surface stay on the free surface. It may be compactly stated as

$$\frac{D(\eta - y)}{Dt} = 0 \quad \text{on } y = \eta(x, y) \quad (2.1.3)$$

(iv) Bernoulli's equation, evaluated on the free surface, is known as the dynamic free surface boundary condition and is written

$$\frac{1}{2} \rho (\nabla \Phi \cdot \nabla \Phi) - \rho g \eta = \text{constant on } y = \eta(x, y) \quad (2.1.4)$$

(v) The governing equation for the flow is Laplace's equation

$$\nabla^2 \Phi = 0 \quad (2.1.5)$$

and it applies at all points within the flow $y > 0$ that are not on a boundary of the flow.

Solution of the exact problem as specified cannot be determined using existing analytic techniques. Specifically, the difficulties are the nonlinearity of the free surface conditions and the imposition of all the boundary conditions on surfaces which are not known a priori, but are rather part of the solution with the exception of the known location of the foil (in the inverse problem).

To render the problem tractable, the free surface condition is linearized and all boundary conditions are satisfied on known surfaces assumed arbitrarily close to the unknown surfaces actually specified. Reduction of the complexity of the boundary conditions is based on the assumption that the perturbation velocities $\{\phi_x, \phi_y, \phi_z\} = \{u, v, w\}$ are small (second order) compared to U , the free stream velocity (first order).

Bypassing the usual steps associated with obtaining a formulation for the perturbation potential, ϕ , the results of this linearization are:

(i) The flow tangency condition is specified on the plane $z = 0$, and the velocity transverse to the flow is

$$\phi_z = -U \frac{\delta z_{me}}{\delta x} \quad \text{on } z = 0 \quad (2.2.1)$$

(ii) The Kutta condition requires that the pressure be constant across the foil at its trailing edge. The linearized pressure is given by Bernoulli's equation.

$$C_p = \frac{P - P_\infty}{\frac{1}{2} \rho U^2} = +2 \phi_x / U \quad (2.2.2)$$

The Kutta condition then states that

$$\phi_x = 0 \quad \text{at the trailing edge } x = 0$$

(iii) The Kinematic free surface condition is:

$$\frac{D}{Dt} (\eta - y) = \frac{\partial \eta}{\partial t} + (u - U) \frac{\partial \eta}{\partial x} + w \frac{\partial \eta}{\partial z} - v = 0 \quad (2.2.3)$$

$$v = \frac{\partial \eta}{\partial t} + (u - U) \frac{\partial \eta}{\partial x} + w \frac{\partial \eta}{\partial z} \quad \text{on } y = 0$$

As the solution is independent of time $\eta_t = 0$.

The terms $u\eta_x$ and $w\eta_z$ are second order and dropped leaving:

$$v = \frac{\partial \phi}{\partial y} = -U \frac{\partial \eta}{\partial x} \quad \text{on } y = 0$$

(iv) The dynamic free surface condition; assuming

$p = 0$ on $y = 0$, and expanding the $\nabla \phi \cdot \nabla \phi$ term is:

$$\frac{1}{2} (\phi_x^2 + \phi_y^2 + \phi_z^2) - g\eta = 0 \quad (2.2.4)$$

$$\frac{1}{2} ((\phi_x - U)^2 + \phi_y^2 + \phi_z^2) - g\eta = 0 \quad \text{on } y = 0$$

keeping only first order terms

$$U \phi_x + g\eta = 0 \quad \text{on } y = 0$$

(v) As before, Laplace's equation:

$$\nabla^2 \phi = 0 \quad (2.2.5)$$

must be satisfied at all interior points in the flow. A combined form of the free surface condition may be formed by eliminating η to give:

$$\phi_y + \frac{U^2}{g} \phi_{xx} = 0 \quad \text{on } y=0 \quad (2.3)$$

III FORMULATION OF THE SOLUTION IN TERMS OF A DIPOLE SHEET

The development of equations relating to the shape of a foil and the hydrodynamic load acting upon it closely parallels the development of lifting surface theory. As in lifting surface theory, an integral equation is established using Green's theorem which states that a potential (here a velocity potential) may be determined everywhere within and on the boundaries of a fluid domain in terms of the potential and its normal derivative on the boundaries. The development of a theory for a lifting surface of zero thickness is found in many texts on classical incompressible subsonic aerodynamics and is not included in the present paper. (An excellent exposition may be found in Ashley and Landahl (10).) The resulting equation is:

$$\phi = -\frac{1}{2\pi} \iint_{\text{wing \& wake}} \Delta\phi \frac{\partial\phi_s}{\partial z_0} dx_0 dy_0 \quad (3.1)$$

where ϕ is the perturbation velocity potential for the flow on the foil, $\Delta\phi = \phi(x,y,0^+) - \phi(x,y,0^-)$ is the difference in value of the potential on adjacent surfaces of the foil, and ϕ_s is the velocity potential for a point source singularity. Noting that $\partial\phi_s/\partial z_0$ is the potential for a dipole whose axis is transverse to the free stream flow, equation 3.1 may be viewed as the convolution of a potential jump distribution $\Delta\phi$ with the "impulse response" of a point potential jump, the dipole. The potentials for a source and a dipole at

(x_0, y_0, z_0) in an infinite fluid are respectively:

$$\phi_s = \frac{1}{r} \quad \phi_d = \frac{z - z_0}{r^3} \quad (3.2)$$

where

$$r = \sqrt{(x - x_0)^2 + (y - y_0)^2 + (z - z_0)^2}$$

When the free surface condition is imposed in the formulation, it is satisfied by utilizing an elemental point dipole potential satisfying the free surface conditions. Many distributions of these dipoles will satisfy the free surface condition as well; a separate section is devoted to developing restrictions which delineate exceptional cases.

Two equivalent formulations for a source in the presence of a free surface are known. In both cases a function, regular in the fluid domain, is added to the potential for a dipole in an infinite fluid, with the two functions collectively satisfying the free surface condition. The first is what may be called the odd image formulation in which the function regular in the fluid domain includes an image sink of equal strength located symmetrically above the plane of the free surface. This potential may be found in many treatises on free surface flows including Wehausen (19) and Peters and Stoker (18). In the present work, a second form is used and may be referred to as the even image formulation as it contains an image source above the plane of the free surface. Following Newman (1) and Wehausen (19)

(equation 13.36), this source potential is:

$$\phi_s = \frac{1}{r} + \frac{1}{r'} - \frac{4}{\pi} \operatorname{Re} \int_0^{\frac{\pi}{2}} \int_0^{\infty} \frac{\lambda}{\lambda - v \sec^2 \theta} \cdot \cos[\lambda(z-z_0) \sin \theta] e^{-\lambda[y+y_0 + i(x-x_0) \cos \theta]} d\lambda d\theta \quad (3.3)$$

where $v = g/U^2$ and x, y, z are temporarily dimensional.

$$r = \sqrt{(x-x_0)^2 + (y-y_0)^2 + (z-z_0)^2}$$

$$r' = \sqrt{(x-x_0)^2 + (y+y_0)^2 + (z-z_0)^2}$$

The source potential given by Wehausen (19) is for the even formulation. In Appendix F this form is shown equivalent to that of equation 3.3.

Nondimensionalizing all lengths with the foil's chord C_0 and the wave number λ with v , ϕ_s may be rewritten:

$$\phi_s = \frac{1}{C_0} \left\{ \frac{1}{r} + \frac{1}{r'} - \frac{4}{\pi} \operatorname{Re} \int_0^{\frac{\pi}{2}} \int_0^{\infty} \frac{kF}{k - \sec^2 \theta} \cdot \cos[kF(z-z_0) \sin \theta] e^{-kF[y+y_0 + i(x-x_0) \cos \theta]} dk d\theta \right\} \quad (3.4)$$

where $F = gC_0/U^2$.

Finally, the corresponding potential for a dipole with axis transverse to the free stream and situated on the plane $z_0 = 0$, is:

$$\phi_d = \frac{1}{c_0} \left\{ \frac{z}{r^3} + \frac{\bar{z}}{r^3} - \frac{4}{\pi} \operatorname{Re} \int_0^{\frac{\pi}{2}} \int_0^{\infty} \frac{(KF)^2}{K - \sec^2 \theta} \cdot \sin(KFz \sin \theta) e^{-KF[y+y_0 + i(x-x_0) \cos \theta]} dK d\theta \right\} \quad (3.5)$$

Now, a potential analogous to equation 3.1 for an infinite fluid, satisfying the linearized conditions (equation 2.2) for a surface piercing hydrofoil may be written:

$$\phi(x, y, z) = -\frac{1}{2\pi} \int_0^{AR} \int_0^1 \Delta \phi(x_0, y_0) \phi_d(x, y, z, x_0, y_0, F) dx_0 dy_0 \quad (3.6)$$

The functional relation between foil loading and shape may be determined by noting that the induced velocity normal to the foil is $\partial\phi/\partial y$, and that the shape of the foil is:

$$z_{me} = z_{me}(1, y) + \int_1^x \frac{\partial \phi}{\partial z} dx_0 \quad (3.7)$$

The loading acting on a foil is specified by $\Delta\phi$ since the circulation from a point on one foil surface to the adjacent point on the other is:

$$\Gamma = \int_{x, y, \sigma^-}^{x, y, \sigma^+} \frac{\partial \phi}{\partial q} \cdot dq = -\Delta\phi \quad (3.8.1)$$

$$\Gamma = - \int_{x,y,0^+}^{x,y,0^-} \phi_{x_0} dx_0 - \int_{x,y,0^-}^{x,y,0^+} \phi_{x_0} dx_0 = -2 \int_{x,y,0^+}^{x,y,0^-} \phi_{x_0} dx_0 \quad (3.8.2)$$

Since the perturbation velocity ϕ_x is odd in z , the contribution from each side $z = 0^\pm$ is equal.

With $\Gamma(x,y)$ known, the local pressure jump can be determined by noting that the local bound vortex density $\gamma(x,y) = -\partial\Gamma/\partial x$. Furthermore, the force on a differential element is $\rho U \gamma(x,y) dx dy$, and the pressure is $\rho U \gamma(x,y)$. For clarity, these results are restated. A positive potential jump $\Delta\phi$ across the foil results when $\phi(x,y,0^+) > \phi(x,y,0^-)$. Integrating $\vec{V} \cdot \vec{dl}$ on a path from $(x,y,0^+)$ to $(x,y,0^-)$, the net circulation for positive $\Delta\phi$ is negative (ϕ_{x_0} is positive on $(x,y,0^+)$ in equation 3.8) and the side force is positive owing to the negative free stream ($U < 0$); the result that the total lift is equal to $\rho U \Gamma_\Gamma$, where Γ_Γ is the total circulation, is negative for $\Delta\phi > 0$, and can be computed by integrating either $\gamma(x,y)$ over the foil or $\Gamma(0,y)$ across the span. Summarizing,

$$\Delta p = p(x,y,0^+) - p(x,y,0^-) = 2\rho U \phi_x(x,y,0^+)$$

$$2 \phi_x(x,y,0^+) = \gamma(x,y) = -\frac{\partial \Gamma}{\partial x}$$

$$\Delta \phi(x,y) = -\bar{\Gamma}(x,y)$$

(3.9)

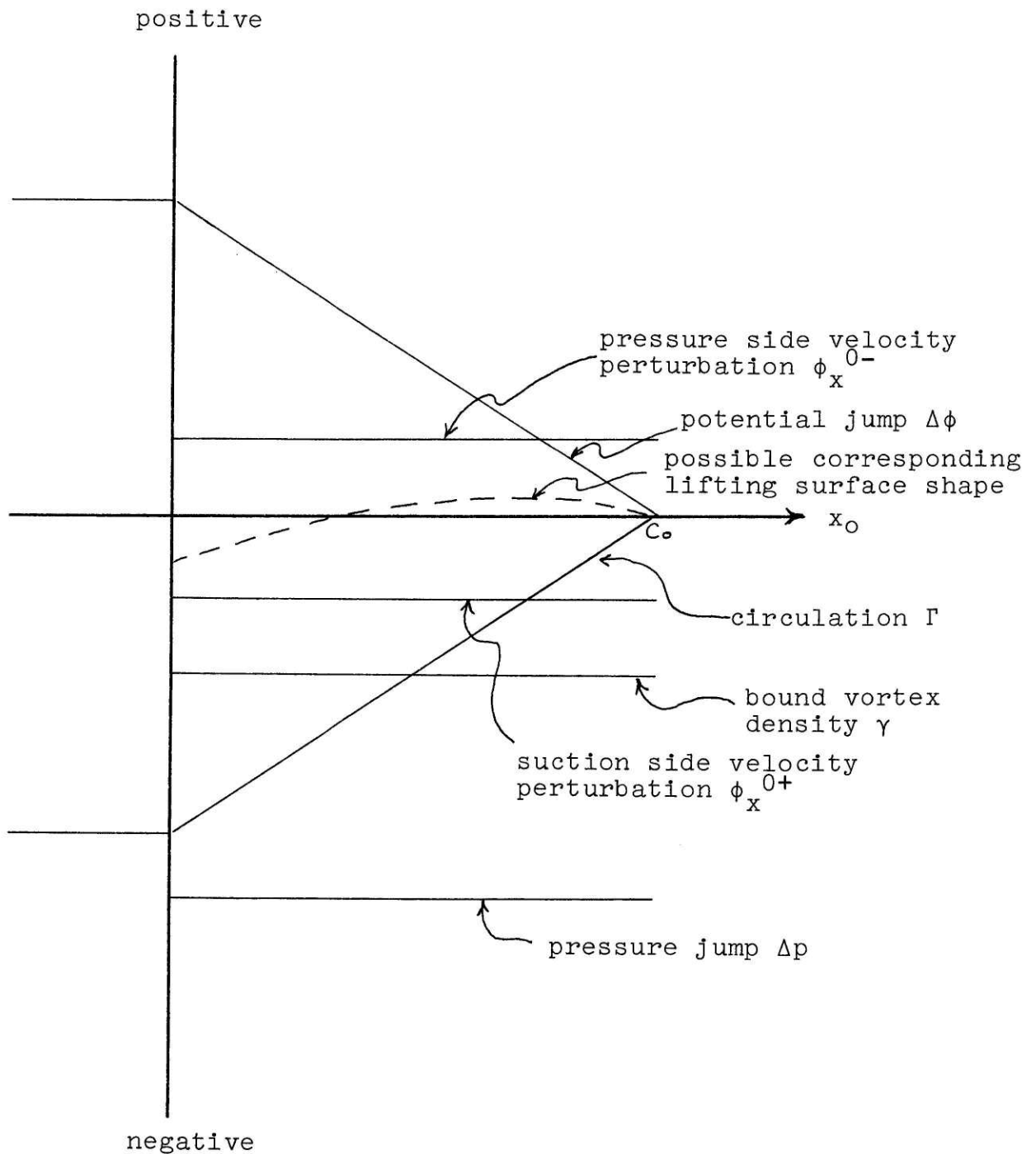


Figure 3 Conventions of positive dipole moment, potential jump, vorticity, side force, circulation and pressure jump

These conventions are illustrated in Figure 3 for the hypothetical case of uniform chordwise loading.

At this point the only modification of the formulation made is to use it to define velocities normal to the foil. Equation 3.6 for ϕ is differentiated with respect to z , and then z is set equal to zero, giving an equation for the "downwash"; a carry over term from airfoil theory where normal velocities on wings are generally in a downward direction. Taking the derivative of ϕ in the z direction within the integral (in this case four integrals) is not always permissible and care must be taken to properly interpret the resulting expression in terms of generalized functions. Formally then:

$$\omega = \left. \frac{\partial \phi}{\partial z} \right|_{z=0} = -\frac{1}{2\pi c_0} \int_0^{AR} \int_{-\infty}^{\infty} \phi(x_0, y_0) \left. \frac{\partial \phi_d}{\partial z} \right|_{z=0} dx_0 dy_0 \quad (3.10)$$

where

$$\left. \frac{\partial \phi_d}{\partial z} \right|_{z=0} = \left\{ \frac{1}{r^3} + \frac{1}{r'^3} - \frac{4}{\pi} \operatorname{Re} \int_0^{\frac{\pi}{2}} \int_0^{\infty} \frac{k^3 F^3}{k - \sec^2 \theta} \sin^2 \theta \cdot e^{-kF[y+y_0 + i(x-x_0)\cos\theta]} dk d\theta \right\}$$

Again following lifting surface theory, the integral equation 3.10, for a surface piercing foil may be reduced to a more compact form by modifying the kernel and reducing the integration limits.

IV THE HORSESHOE VORTEX INTEGRAL EQUATION FORMULATION

The integral equation 3.10 for a dipole sheet is restated with $\Delta\phi(x_0, y_0)$, the local dipole sheet strength, replaced with $\Gamma(x_0, y_0)$ to clarify following developments.

$$\phi(x, y) = \frac{1}{2\pi} \int_0^{AR} \int_0^1 \Gamma(x_0, y_0) \phi_d(x, y, x_0, y_0, F) dx_0 dy_0 \quad (4.1)$$

Certain physical arguments may be used to compact the region over which the Green's function ϕ_d must be integrated. As a first step, pressure jumps across the wake ($x < 0$, $0 \leq y \leq AR$) may be ruled out on the physical ground that an unrestrained pressure discontinuity would result in infinite fluid particle accelerations. A streamwise increase (or decrease) of $\Gamma(x_0, y_0)$ in the wake corresponds to a local increase (or decrease) in the (vertical) vorticity in the flow which must be zero not to produce an unacceptable pressure jump. It can therefore be stated that $\partial\Gamma/\partial x_0$ is zero in the wake region $-\infty < x_0 \leq 0$. (A possible exception on the plane of the free surface exists and is discussed in Appendix E.) With this result, the integration bounds in equation 4.1 can be reduced to include simply the foil's planform ($0 \leq y_0 \leq AR$, $0 \leq x_0 \leq 1$). This is accomplished by integrating by parts once in the x_0 direction; details of the derivation are set

forth in Appendix A. The resulting expression for the downwash is:

$$\omega(x,y) = \frac{1}{2\pi c_o} \int_0^{AR} \int_0^1 \gamma(x_o, y_o) G(x,y, x_o, y_o, \bar{r}) dx_o dy_o$$

$$G = -\frac{1}{(y-y_o)^2} \left\{ 1 - \frac{x-x_o}{\sqrt{(x-x_o)^2 + (y-y_o)^2}} \right\}$$

$$- \frac{1}{(y+y_o)^2} \left\{ 1 - \frac{x-x_o}{\sqrt{(x-x_o)^2 + (y+y_o)^2}} \right\}$$

$$+ \frac{4}{\pi} \text{Im} \int_0^{\frac{\pi}{2}} \int_0^{\infty} \frac{k^2 F^2}{k - \sec^2 \theta} \tan \theta \sin \theta \cdot$$

$$e^{-kF [y+y_o + i(x-x_o) \cos \theta]} dk d\theta \quad (4.2)$$

where $\gamma(x_o, y_o)$ is the bound vortex sheet strength and is equal to $-\partial\Gamma(x_o, y_o)/\partial x_o$, and the integral sign with the X signifies that the integral be evaluated using Mangler's "recipe" as set forth in Ashley and Landahl (10), pp. 130-131.

Newman (1) has carried the analysis directly from the dipole sheet form to one which can be obtained by partially integrating the above horseshoe formulation over the y_o direction. The nonkernel part of the integrand is then $\partial^2\Gamma/\partial x_o \partial y_o$ and the kernel is found to represent a point increase in free vorticity. This form is analogous to that of Robinson and Lauerman (6) for a lifting surface in an infinite fluid. It does not, however, yield any further reduction of the integral bounds and slightly increases the complexity of the kernel.

It is included in Appendix C for completeness; no future use of it is made herein.

Before proceeding toward a solution of equation 4.2 for a surface piercing foil of arbitrary loading or shape, three limiting cases are discussed to place the general case in perspective. They are the limits of zero and infinite Froude number and infinite aspect ratio (lifting line).

V THE ZERO FROUDE NUMBER ($F \rightarrow \infty$) LIMIT

In his thesis, Letcher (17) makes an observation helpful to those not thoroughly imbued with the concept of Froude numbers. It is that when visualizing a limiting Froude number case, it is often best to imagine that variations of the acceleration of gravity cause the effect rather than variations of the length scale or velocity which are generally more physically apparent and with which one might associate nonFroude number effects. (For example, Reynolds number effects with velocity variation.)

The cases of zero and infinite F can be analyzed with decreasing degrees of mathematical rigor depending upon how early in the formulation the limit is taken. For $F_n \rightarrow 0$, g can be imagined to tend to infinity with U and the length scale C_0 fixed. From the combined free surface boundary condition it can be seen that as $g \rightarrow \infty$ with U held constant, ϕ_y must tend to zero since ϕ_{xx} must remain finite as physical arguments require. Thus, the anticipated limit as $F_n \rightarrow 0$ is one satisfying a boundary condition $\phi_y = 0$ on $y = 0$ and physical corresponds to a foil of span $2S_0$ in an infinite fluid. In equation 4.2 this corresponds to the double integral portion of the kernel vanishing as $F_n \rightarrow 0$. Letting $KF = \lambda$, this expression becomes

$$-\frac{4}{\pi} \text{Im} \int_0^{\frac{\pi}{2}} \int_0^{\infty} \frac{\lambda^2 \tan \theta \sin \theta}{\lambda - F \sec^2 \theta} \cdot e^{-\lambda [y + y_0 + i(x - x_0) \cos \theta]} d\lambda d\theta \quad (5.1)$$

which tends to zero for $F \rightarrow \infty$ ($F_n \rightarrow 0$). The integral equation 4.2 thus reduces to the familiar integral equation for a lifting surface of span $2AR$ and may be written:

$$w(x,y) = -\frac{1}{2\pi c_0} \int_{-AR}^{AR} \int_0^1 \gamma(x_0, y_0) \frac{1}{(y-y_0)^2} \left\{ 1 - \frac{x-x_0}{\sqrt{(x-x_0)^2 + (y-y_0)^2}} \right\} dx_0 dy_0$$

(5.2)

VI THE INFINITE FROUDE NUMBER LIMIT ($F \rightarrow 0$)

Following the same lines of thought as in developing the zero Froude number limit, the infinite Froude number limit is considered to be the result of the gravitational acceleration tending to zero. From the combined free surface boundary condition one finds that the new boundary condition on $y = 0$ is that $\phi_{xx} = 0$. Since $\phi \rightarrow 0$ for all z at $x = +\infty$, this condition is equivalent to the condition that $\phi = 0$ everywhere on the plane $y = 0$. Considering the formulation for the potential rather than the downwash, it can be seen that the proper limiting form of the Green's function is one in which the nonintegral terms form an odd pair whose contributions to the potential exactly cancel on the surface $y = 0$. Had the present formulation been founded on the Green's function for a source with its odd image, the present task would be to demonstrate that, after having been manipulated into the Green's function for the downwash due to a horseshoe vortex, the double integral part of kernel vanishes in the limit of $F_n \rightarrow \infty$.

Conversely, it must now be shown that the double integral term is such that when its infinite Froude number limit is added to the even image, the resulting kernel contains the desired negative image. Using the form of the double integral term in equation 4.2, and separating the residue I_r and Cauchy Principle I_{pv} value contributions:

$$\begin{aligned}
\bar{I}_R &= -\frac{4}{\pi} \operatorname{Im} \int_0^{\frac{\pi}{2}} \pi i F^2 \sec^2 \theta \tan \theta \sin \theta \cdot \\
&\quad e^{-F \sec^2 \theta [(y+y_0) + i(x-x_0) \cos \theta]} d\theta \\
&= -4F^2 \int_0^{\frac{\pi}{2}} \sec^2 \theta \tan \theta \sin \theta \cos [F \sec \theta (x-x_0)] \cdot \\
&\quad e^{-F \sec^2 \theta (y+y_0)} d\theta
\end{aligned} \tag{6.1}$$

Here the order of performing the integration first and then taking the limit is important. For any finite value of $F(y + y_0)$, the integral is convergent as $\theta \rightarrow \pi/2$. The subsequent limit as $F \rightarrow 0$ then properly assigns a value of zero to the residue contribution. The Cauchy Principle value contribution is:

$$\bar{I}_{PV} = \frac{4}{\pi} \int_0^{\frac{\pi}{2}} \int_0^{\infty} \lambda \tan \theta \sin \theta \sin [\lambda (x-x_0) \cos \theta] \cdot \\
e^{-\lambda (y+y_0)} d\lambda d\theta \tag{6.2}$$

where the pole has been absorbed by a second order zero at the origin. In Appendix C this integral is shown to equal:

$$\bar{I}_{PV} = -\frac{2}{(y+y_0)^2} \left\{ 1 - \frac{x-x_0}{\sqrt{(x-x_0)^2 + (y+y_0)^2}} \right\}$$

The formulation for infinite Froude number may thus be written:

$$\omega(x, y) = -\frac{1}{2\pi c_0} \int_0^{AR} \int_0^1 \gamma(x_0, y_0) \left\{ \frac{1}{(y-y_0)^2} \left[1 - \frac{x-x_0}{\sqrt{(x-x_0)^2 + (y-y_0)^2}} \right] - \frac{1}{(y+y_0)^2} \left[1 - \frac{x-x_0}{\sqrt{(x-x_0)^2 + (y+y_0)^2}} \right] \right\} dx_0 dy_0 \quad (6.3)$$

In passing it should be noted that the vanishing contribution from the residue portion of the integral in the kernel might have been anticipated because that part of the integral represents a three dimensional radiated surface wave. Passing to the limit of infinite Froude number, there no longer remains a mechanism for the transmission of gravity waves as to do so there must be a means of storing potential energy. Since in the limit of infinite Froude number, a wave cannot propagate in the medium, it is apparent that no contribution should be made by the residue term.

VII LIFTING LINE THEORY

Lifting line theory is an approximate theory for wings whose chords are small compared to their spans. Physically, the simplifying assumption states that the induced normal velocity on the wing is dominated by the trailing vorticity in the wake and that the effect of bound vorticity can be neglected. The corresponding mathematical statement is that the bound vorticity $\gamma(x_0, y_0)$ is distributed in the chordwise direction as a Dirac delta function. Thus,

$$\gamma(x_0, y_0) = \delta(x_0) \Gamma'(y_0) \quad (7.1)$$

When substituted into the integral equation 4.2 and integrated with respect to x_0 , the delta function selects the value of the integrand at $x_0 = 0$. The result is a simplified integral equation for the downwash on the lifting line $x = y = 0$:

$$w(0, y) = -\frac{1}{2\pi c_0} \int_0^{AR} \Gamma'(y_0) \left\{ \frac{1}{(y+y_0)^2} + \frac{1}{(y-y_0)^2} \right. \quad (7.2)$$

$$\left. - \frac{4}{\pi} \operatorname{Im} \int_0^{\frac{\pi}{2}} \int_0^{\infty} \frac{(kF)^2}{k - \sec^2 \theta} \sin \theta \tan \theta e^{-kF(y+y_0)} dk d\theta \right\} dy_0$$

Because the chord has been set to zero for the lifting line limit, modifications must be made to the nondimensionalization of the equations. Returning to dimensional space variables, taking F as a parameter of dimension (1/length)

and AR as the dimensional span gives the proper interpretation. These all follow if the chord length C_0 is taken as dimensionless unity wherever it appears.

The only imaginary contribution from the double integral in the kernel arises from the residue and is:

$$I = -4F^2 \int_0^{\frac{\pi}{2}} \tan^2 \theta \sec^3 \theta e^{-F \sec^2 \theta (y+y_0)} d\theta \quad (7.3)$$

This can be integrated analytically to give:

$$I = -\frac{F}{y+y_0} e^{-\frac{F}{2}(y+y_0)} K_1 \left(\frac{F}{2}(y+y_0) \right) \quad (7.4)$$

where K_1 is the modified Bessel function of the first kind, order one. The complete equation for a surface piercing lifting line may then be written as:

$$w(o,y) = -\frac{1}{2\pi c_0} \int_0^{AR} \Gamma(y_0) \left[\frac{1}{(y+y_0)^2} + \frac{1}{(y-y_0)^2} - \frac{F}{y+y_0} e^{-\frac{F}{2}(y+y_0)} K_1 \left(\frac{F}{2}(y+y_0) \right) \right] dy_0 \quad (7.5)$$

For small argument q , K_1 may be approximated by

$$K_1(q) \cong \frac{1}{q} + \frac{q}{2} \ln \frac{q}{2} + \dots$$

and the contribution to the downwash by the loading in the vicinity of $y_0 = 0$ is:

$$\omega(o, y) = -\frac{1}{2\pi c_o} \int_0^\epsilon \Gamma(y_o) \left\{ \frac{1}{(y-y_o)^2} - \frac{1}{(y+y_o)^2} - \frac{F^2}{4} \ln \left(\frac{F}{4} (y+y_o) \right) \right\} dy_o \quad (7.6)$$

where ϵ is some small positive number such that for $0 \leq y_o < \epsilon$ the approximation of K_1 is valid.

For the downwash on the lifting line near the free surface due to loading near the free surface, the integral equation indicates that locally the behavior is identical to an odd image or infinite Froude number formulation.

A primary goal of the present research has been to determine necessary conditions on the spanwise (vertical) load distribution which suffice to preclude infinite perturbations of the velocity on the free surface. The semblance between proximity of the free surface and infinite Froude number is central to the resolution of this matter, which is discussed in a later section.

For the integral equation 7.6 above, conditions on the circulation $\Gamma(y_o)$ necessary to insure bounded downwashes on the lifting line are the same as have been obtained by Betz and Peterson (21) for a lifting line and its reversed circulation image. The same result has been obtained by an alternate method in Appendix D and is that:

$$\Gamma(y_o) \sim O(y_o \ln y_o) \text{ as } y_o \rightarrow 0$$

VIII PERMISSIBLE LOADINGS

With the eventual goal of solving either the direct or inverse problem by means of linearly superposing downwashes associated with assumed loading modes, it is essential to understand precisely the conditions imposed on loadings necessary to insure finite downwash on the free surface. Acceptable loadings must satisfy conditions arising from both the infinite fluid horseshoe vortex (and its image) portion of the kernel and the double integral contribution to the kernel.

First, consider the contribution of the algebraic terms in the kernel corresponding to the zero Froude number, double aspect ratio formulation. By considering the downwash far downstream in the wake, it can be shown that the loading at the plane of the free surface must have zero first derivative with respect to y_0 . Noting first that loading below the free surface plane is evenly mirrored above the plane and second, that the derivative of an even function is an odd function, it can be seen that if the derivative of the vertical (spanwise) loading does not tend to zero as $y \rightarrow 0^+$, there will be a discontinuity in the derivative of the spanwise loading across the plane of the free surface. Since the strength of the trailing vortex sheet is equal to the derivative of the spanwise loading, it also will be discontinuous at the plane of the free surface if the vertical load's derivative is nonzero. It can easily be seen that the discontinuity of this

vortex sheet strength precludes the usual principal value integral cancellation at the discontinuity and gives rise to a logarithmic singularity in the downwash

$$\omega(y) = \int_{-AR}^{AR} \frac{\delta\Gamma}{\delta y_0} \cdot \frac{1}{y-y_0} dy_0 \quad (8.1)$$

if at the surface $y = 0$, $\partial\Gamma/\partial y_0$ is discontinuous. The contribution to the downwash from the immediate ϵ vicinity of the free surface is

$$\omega(0) = -2 \int_0^\epsilon \frac{\delta\Gamma}{\delta y_0} \frac{1}{y-y_0} dy_0 = -2 \frac{\delta\Gamma(0^+)}{\delta y_0} \ln(y)$$

$$\text{if } \frac{\delta\Gamma(0^+)}{\delta y_0} = - \frac{\delta\Gamma(0^-)}{\delta y_0} \quad (8.2)$$

In summary, the portion of the kernel consisting of the horseshoe and its positive image imposes a restriction of zero derivative of the loading (circulation or bound vortex sheet strength) at the plane of the free surface.

The contribution to the downwash from the double integral term in the kernel cannot be properly assessed far downstream (as was done for the other terms) because three dimensional wave radiation effects preclude the downstream reduction to two dimension (Trefftz plane) flow. (Far downstream the downwash from the double integral term in fact vanishes due to cancellation effects of the highly oscillatory integrand.)

Proper assessment of the double integral's contribution can be made by reversing the orders of integration to first integrate over the foil's planform. Defining the Laplace transform of the spanwise loading and the Fourier transform of the chordwise loading as,

$$\bar{Y}(\lambda) = \int_0^{AR} Y(y_0) e^{-\lambda y_0} dy_0 \quad (8.3.1)$$

$$\bar{X}(p\lambda) = \int_0^1 X(x_0) e^{i\lambda p x_0} dx_0 \quad (8.3.2)$$

$$Y(x_0, y_0) = Y(y_0) X(x_0) \quad (8.3.3)$$

the double integral contribution in equation 4.2 (with $\lambda = KF$ and $p = \cos \theta$) becomes

$$\omega_\omega(x, y) = -\frac{2}{\pi^2} \frac{I_m}{c_0} \int_0^1 \int_0^\infty \bar{X}(p\lambda) \bar{Y}(\lambda) \frac{\lambda^2}{p^2\lambda - F} \cdot p \sqrt{1-p^2} e^{-\lambda[y + i x p]} d\lambda dp \quad (8.4)$$

For the downwash to remain finite for all finite F and y (and in the limit as $y \rightarrow 0$) a sufficient condition is that the product $\bar{X}\bar{Y}$ be $o(1/\lambda^2)$ as $\lambda \rightarrow \infty$. This may be shown by considering the absolute convergence of the λ integral in equation 8.4. Considering only the contribution to the λ integral from some large $\lambda = B \gg F/p^2$ to $\lambda = \infty$;

$$I = \int_B^\infty \bar{X}(p\lambda) \bar{Y}(\lambda) \frac{\lambda^2}{p^2\lambda - F} e^{-\lambda[y + i x p]} d\lambda \quad (8.5.1)$$

$$I \approx \frac{1}{\rho^2} \int_B^{\infty} \bar{X}(\rho\lambda) \bar{Y}(\lambda) \lambda e^{-\lambda[y + i x \rho]} d\lambda \quad (8.5.2)$$

If the product $\bar{X}\bar{Y}$ tends to zero as $\lambda^{-\beta}$ for $\lambda \rightarrow \infty$, the integral will converge only if $\beta > 2$ such that the integrand will be $O(\lambda^{-\beta+1})$ and its improper integral will decay like $\lambda^{-\beta+2}$.

Since for any $\beta > 2$, the integral (8.5.2) converges, the loading $\bar{X}(\rho\lambda)\bar{Y}(\lambda)$ must be $o(1/\lambda^2)$. In the delimiting case, $\bar{X}(\rho\lambda)\bar{Y}(\lambda) \sim O(1/\lambda^2)$ as $\lambda \rightarrow \infty$, the integrand tends to zero as $1/\lambda$ as $\lambda \rightarrow \infty$ and a logarithmic singular in the downwash at the free surface results.

It seems highly unlikely that the independent logarithmic singularities in the downwash at the free surface from the double integral term and from the infinite fluid and image terms cancel because the double integral term's contribution must decay far downstream for any nonzero finite F whereas the infinite fluid terms tend toward two dimensional flow. In addition, the magnitude of the double integral term contribution is dependent on F while the other contributions are not, and exact cancellation of the logarithmic singularities cannot be generally expected.

In summary, for surface piercing hydrofoils of arbitrary finite aspect ratio operating at any finite nonzero Froude number, two restrictions on load distributions are imposed. First, the derivative of the load at the free surface must be

zero; second, the product of the loading transforms $\bar{X}(p\lambda)\bar{Y}(\lambda)$ must be $O(1/\lambda^2)$ as $\lambda \rightarrow \infty$.

It will be recalled that the previously obtained formulation for the lifting line case indicated that the downwash on the lifting line would remain finite if the loading was $O(y_0 \ln y_0)$ as $y_0 \rightarrow 0$. This clearly violates the conditions imposed on lifting surfaces since not only is the vertical derivative of the load infinite, but product of the loading transforms:

$$\bar{X}(p\lambda) = \int_0^1 \delta(x_0) e^{i\lambda p x_0} dx_0 = 1 \quad (8.6.1)$$

$$\bar{Y}(\lambda) = \int_0^\infty y_0 \ln y_0 e^{-\lambda y_0} dy_0 = \frac{1}{\lambda^2} \left[2 - \ln(\gamma' \lambda) \right] \quad (8.6.2)$$

$\gamma' = \text{Euler's constant}$

decays only as $O(\ln \lambda / \lambda^2)$ as $\lambda \rightarrow \infty$. (Here the spanwise transform has been integrated to infinity for simplicity as the result is sought only for large λ , and as $\lambda \rightarrow \infty$ only the behavior of the loading in the immediate vicinity of the free surface affects the transform.)

This apparent contradiction may be resolved by noting that in the development for a lifting line, only the downwash on the lifting line itself is examined. It was found that on the lifting line the only double integral term contribution to the downwash arises from the residue and is a radiated wave effect. The downwash resulting from the near field (Cauchy principle value integral) contribution, although zero on the lifting line is unbounded as the free surface is approached elsewhere on the track $z = 0$ for some loadings.

In lifting surface theory this infinity of the downwash could not be tolerated because the foil occupied a finite portion of the track on the free surface and an infinite downwash (excepting integrable infinities at discrete points across the chord) would imply an unrealizable foil shape. For lifting line theory, however, this difficulty does not arise because the theory does not (and is not expected to) satisfy body boundary conditions on a foil. It is rather a theory for an outer region far from the foil, whose inner limit gives the downwash on a high aspect ratio foil induced by trailing vorticity in its wake. Whether the infinite velocity induced on the free surface track $z = 0$ extends over the entire free surface is not known. Furthermore, the acceptability of this infinity in terms of the amount of kinetic energy per unit distance downstream (and therefore work done by the foil) remains to be investigated.

In summary, the lifting line high aspect ratio theory need not require finite transverse perturbation velocities to assure attainable foil shapes, but must not permit infinities which lead to infinite kinetic energy per unit distance downstream in the wake as this corresponds to a physically unacceptable infinite drag force. It is apparent that the conditions imposed in lifting surfaces theory (the transform of the load being $o(1/\lambda^2)$ as $\lambda \rightarrow \infty$ and the derivative of the vertical load being zero) are stronger than

required for lifting line theory, but further investigations are needed to ascertain whether vertical loadings as singular as $y \ln y$ are permissible.

IX LOADING MODES

A standard lifting surface theory technique for the inverse problem is to assume a series of loading modes, calculate the downwash from each mode at selected points on the planform, and solve a linear matrix equation for the strengths of the various modes required to produce the known downwash (the boundary condition on the wing). Experience has shown that a series of chordwise and spanwise modes known as the Glauert Series rapidly converge for most wing shapes. The loadings in this series are:

$$X(x_o) = a_o \sqrt{\frac{x_o}{1-x_o}} + \sum_{n=1}^{\infty} a_n \sin n \phi_{c_o} \quad (9.1.1)$$

$$Y(y_o) = \sum_{n=1}^{\infty} b_n \sin n \phi_{sp} \quad (9.1.2)$$

where the angles ϕ_{sp} and ϕ_{c_o} are related to y_o and x_o and x_o^* are shown on Figure 4. The first chordwise mode, the a_o term, corresponds to a two dimensional flat plate; the second, a_1 , gives a parabolic meanline. Higher chordwise modes do not affect the total load and serve only to shift the distribution of chordwise load fore and aft. Likewise, the first spanwise mode (elliptical) gives all the lift and higher modes tend only to modify the spanwise lift distribution. The transforms of the first two Glauert chordwise modes and the first Glauert spanwise mode are given below. In addition, several modes whose transforms are particularly well behaved are given.

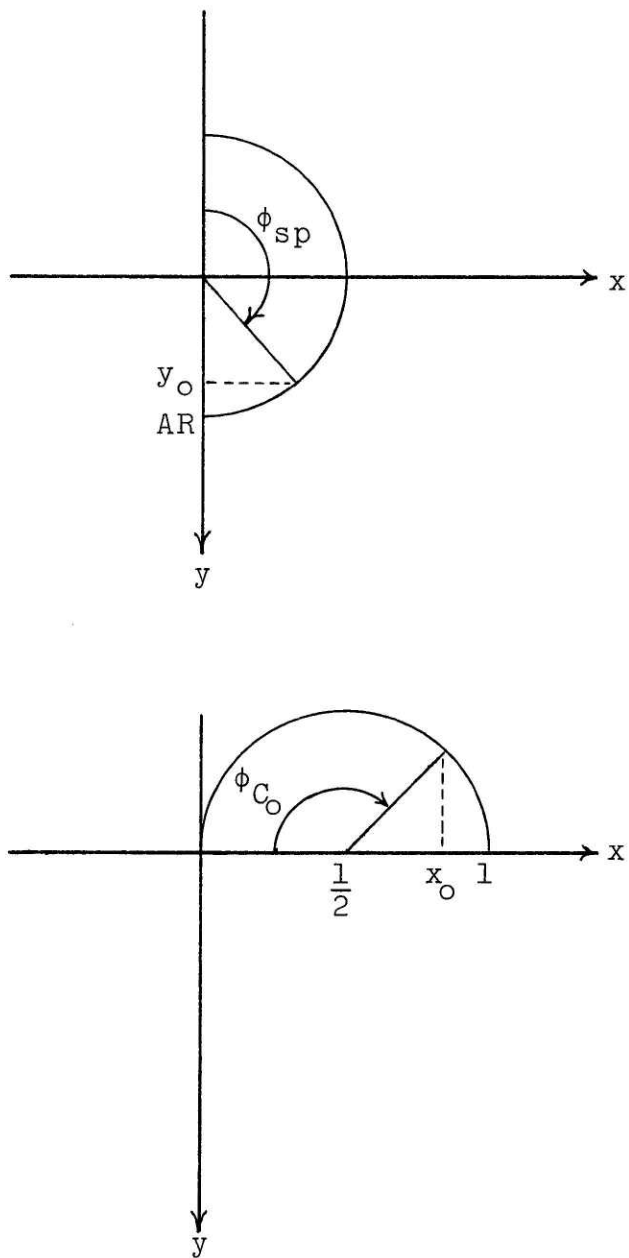


Figure 4 Glauert series mode angle definitions

TABLE 1
Spanwise Modes

1. Elliptical: first Glauert series term

$$Y(y_0) = \frac{4}{\pi AR^2} \sqrt{AR^2 - y_0^2}$$

$$\bar{Y}(\lambda) = 2/AR\lambda [I_1(AR\lambda) - L_1(AR\lambda)]$$

$$\bar{Y}(\lambda) \sim O(1/\lambda^{3/2}) \text{ as } \lambda \rightarrow \infty$$

$$\bar{Y}(0) = 1$$

2. Modified Elliptical:

$$Y(y_0) = \frac{16}{AR^3\pi} y_0 \sqrt{y_0(AR - y_0)}$$

$$\bar{Y}(\lambda) = \frac{4}{AR\lambda} \left[I_1\left(\frac{AR}{2}\lambda\right) + I_2\left(\frac{AR}{2}\lambda\right) \right] e^{-\frac{AR}{2}\lambda}$$

$$\bar{Y}(\lambda) \sim O(1/\lambda^{3/2}) \text{ as } \lambda \rightarrow \infty$$

$$\bar{Y}(0) = 1$$

3. Sinusoid squared:

$$Y(y_o) = \frac{2}{AR} \sin^2 \left(\frac{\pi}{AR} y_o \right)$$

$$\bar{Y}(\lambda) = \frac{4\pi^2}{AR^3} (1 - e^{-AR\lambda}) \frac{1}{\lambda(\lambda^2 + 4\pi^2/AR^2)}$$

$$\bar{Y}(\lambda) \sim O(1/\lambda^3) \quad \text{as } \lambda \rightarrow \infty$$

$$\bar{Y}(0) = 1$$

4. Cubic spanwise:

$$Y(y_o) = 12y_o^2(AR - y_o)$$

$$\bar{Y}(\lambda) = \frac{12}{\lambda} \left[e^{-AR\lambda} \left(\frac{AR^2}{\lambda} + \frac{4AR}{\lambda^2} + \frac{6}{\lambda^3} \right) + \frac{2AR}{\lambda^2} - \frac{6}{\lambda^3} \right]$$

$$\bar{Y}(\lambda) \sim O(1/\lambda^3) \quad \text{as } \lambda \rightarrow \infty$$

$$\bar{Y}(0) = 1$$

TABLE 2
Chordwise Modes

1. Flat plate loading:

$$X(x_0) = \frac{2}{\pi} \sqrt{\frac{x_0}{1-x_0}}$$

$$\bar{X}(\lambda p) = e^{-i\lambda p} [J_0(\lambda p) + i J_1(\lambda p)]$$

$$\bar{X}(\lambda p) \sim O(1/\sqrt{\lambda p}) \quad \text{as } \lambda p \rightarrow \infty$$

$$\bar{X}(0) = 1$$

2. Elliptical loading:

$$X(x_0) = \frac{8}{\pi} \sqrt{x_0} \sqrt{1-x_0}$$

$$\bar{X}(\lambda p) = \frac{2}{\lambda p} J_1(\lambda p) e^{i\lambda p}$$

$$\bar{X}(\lambda p) \sim O(1/(\lambda p)^{3/2}) \quad \text{as } \lambda p \rightarrow \infty$$

$$\bar{X}(0) = 1$$

3. Parabolic loading:

$$X(x_0) = 6x_0(1 - x_0)$$

$$\bar{X}(\lambda p) = \frac{3}{\lambda p} e^{i\lambda p} \left[\frac{\sin \lambda p}{(\lambda p)^2} - \frac{\cos \lambda p}{\lambda p} \right]$$

$$\bar{X}(\lambda p) \sim O(1/(\lambda p)^2) \quad \text{as } \lambda p \rightarrow \infty$$

$$\bar{X}(0) = 1$$

X MODIFICATION OF THE FORMULATION FOR NUMERICAL CALCULATIONS

Rewriting the integral equation for the downwash 4.2 to include the developments (for the double integral) of equation 8.4, the formulation becomes:

$$\begin{aligned}
 w(x,y) = & -\frac{1}{2\pi c_o} \int_0^{AR} \int_0^1 \gamma(x_o, y_o) \left\{ \frac{1}{(y-y_o)^2} \left[1 - \frac{x-x_o}{\sqrt{(x-x_o)^2 + (y-y_o)^2}} \right] + \frac{1}{(y-y_o)^2} \left[1 - \frac{x-x_o}{\sqrt{(x-x_o)^2 + (y+y_o)^2}} \right] \right\} dx_o dy_o \\
 & + \frac{2}{\pi^2} \frac{I_m}{c_o} \int_0^1 \int_0^\infty \bar{X}(p\lambda) \bar{Y}(\lambda) \frac{\lambda^2 p}{p^2 \lambda - F} \sqrt{1-p^2} e^{-\lambda(y+ixp)} d\lambda dp \quad (10.1)
 \end{aligned}$$

where as before $\gamma(x_o, y_o) = X(x_o)Y(y_o)$ and $\{\bar{X}, \bar{Y}\}$ are the transforms of the loadings as defined in equations 8.3.

The first integral in the above equation can be seen to be the equation for a lifting surface of aspect ratio $2AR$ in an infinite fluid and may be rewritten:

$$\begin{aligned}
 w_{2AR}(x,y) = & -\frac{1}{2\pi c_o} \int_{-AR}^{AR} \int_0^1 \gamma(x_o, y_o) \cdot \frac{1}{(y-y_o)^2} \left\{ 1 - \frac{x-x_o}{\sqrt{(x-x_o)^2 + (y-y_o)^2}} \right\} dx_o dy_o \quad (10.2)
 \end{aligned}$$

To calculate the downwash $w_{2AR}(x,y)$ due to a loading $\gamma(x_o, y_o)$, the continuous loading is approximated by taking the loading to be concentrated at equally spaced chordwise positions.

The resulting "vortex lattice" formulation, proposed by Faulkner (3), has been successfully employed by Milgram (4) in the study of yacht sails. Accurate results near the center of a wing's span and thus near the plane of the free surface are attained using this method. A short computer program has been written to calculate downwashes W_{2AR} using this vortex lattice technique.

The second integral contribution to the downwash in equation 10.1 gives the perturbation from the zero Froude number limit representing both bound and radiated wave effects. A change of variables and a factorization of the load transforms facilitates the numerical integration. Modified transforms are assumed such that:

$$\bar{X}(p\lambda) = \frac{1}{p\lambda} \bar{X}_m(p\lambda) \quad (10.3.1)$$

$$\bar{Y}(\lambda) = \frac{1}{\lambda} \bar{Y}_m(\lambda) \quad (10.3.2)$$

Letting $p = \sin \theta$, the second expression in 10.1 becomes:

$$W_w(x,y) = \frac{2}{\pi^2 c_0} \text{Im} \int_0^{\frac{\pi}{2}} \int_0^{\infty} \frac{\bar{X}_m(\lambda \sin \theta) \bar{Y}_m(\lambda)}{\lambda \sin^2 \theta - F} \cdot \cos^2 \theta e^{-\lambda(y + ix \sin \theta)} d\lambda d\theta \quad (10.4)$$

Taking the imaginary part,

$$\begin{aligned}
 w_w(x,y) = \frac{2}{\pi^2 c_0} \int_0^{\frac{\pi}{2}} \cos^2 \theta \left\{ \int_0^{\infty} \frac{e^{-\lambda y} \bar{Y}_m(\lambda)}{\lambda \sin^2 \theta - F} \cdot \right. \\
 \left. \left[\cos(x\lambda \sin \theta) \cdot \text{Im} \bar{X}_m(\lambda \sin \theta) - \sin(x\lambda \sin \theta) \cdot \right. \right. \\
 \left. \left. \text{Re} \bar{X}_m(\lambda \sin \theta) \right] d\lambda + \pi e^{-\frac{Fy}{\sin^2 \theta}} \bar{Y}_m\left(\frac{F}{\sin^2 \theta}\right) \cdot \right. \\
 \left. \left[\cos\left(\frac{Fx}{\sin \theta}\right) \cdot \text{Re} \bar{X}_m\left(\frac{F}{\sin^2 \theta}\right) + \sin\left(\frac{Fx}{\sin \theta}\right) \cdot \right. \right. \\
 \left. \left. \text{Im} \bar{X}_m\left(\frac{F}{\sin^2 \theta}\right) \right] \right\} d\theta \quad (10.5)
 \end{aligned}$$

A computer program has been written to evaluate this expression for finite nonzero F and any permissible loading. The inner integral over λ is truncated at a value of λ beyond which the contribution to the integral can be shown to be negligible. This follows for points below the free surface from the effect of the decaying exponential and for points on the free surface from the decay of the pole and the loading's transform (under the present notation $\bar{X}_m(\lambda)\bar{Y}_m(\lambda) \sim 0(1)$ as $\lambda \rightarrow \infty$).

XI NUMERICAL RESULTS

Two loadings have been numerically investigated. They were chosen as representative of two basic loading forms: those with and those without loading at the plane of the free surface. In both cases the chordwise loading was taken to be elliptical. For load extending to the surface, the elliptical spanwise loading was chosen, and for no load at the surface the cubic spanwise mode was used. (See definitions in Tables 1 and 2.) In all cases the calculations are for a negative unit total circulation such that the lift force acts to port (positive z direction) and is of magnitude ρU . The choice of aspect ratio for all loadings was somewhat arbitrarily taken as three, and the effect of varying aspect ratio has not been studied. Finally, the effect of the free surface was anticipated to be significant only near the free surface and has been studied only in this vicinity.

Figures 5 and 6 show the computed downwashes and shapes for an elliptical spanwise and chordwise loading. At zero Froude number the shape can be seen to contain both the camber effect of the bound vorticity and the induced angle of attack effect of the trailing and free vorticity systems. As the Froude number increases from 0.0 to 0.2, the most dramatic effect is the reversal of the sign of the induced angle of attack. The effect continues to grow as the Froude number increases to 0.5, where a reduction in camber becomes apparent.

Both effects continue to develop up to a Froude number of 0.8. Beyond a Froude number of .8, however, the induced angle increases with Froude number and returns to values of the same sign as occur in the zero Froude number limit. In terms of the known infinite Froude number limit, this result could have been anticipated since in this limit the effect of the free surface is to increase the magnitude of the downwash on the foil. (In the infinite Froude number limit the proper image above the plane of the free surface is a foil lifting in the direction opposite that of the actual foil, and the actual foil operates in the "upwash" of the image foil.)

The second loading, cubic spanwise with zero load and zero derivative of vertical load distribution at the free surface, generates a downwash whose variations with Froude number are similar to those for the elliptical spanwise loading. This is particularly interesting since at zero Froude number, the downwash from this loading differs significantly from that of the elliptical loading case. Here, at zero Froude number, there is an upwash near the plane of the free surface due to dominate free and trailing vortex effects of the load concentration near the foil's tip. As may be seen in Figures 7 and 8, the velocities induced at the same depth below the free surface by this loading are an order of magnitude greater than those induced by elliptical spanwise loading. Like the zero Froude number case, it

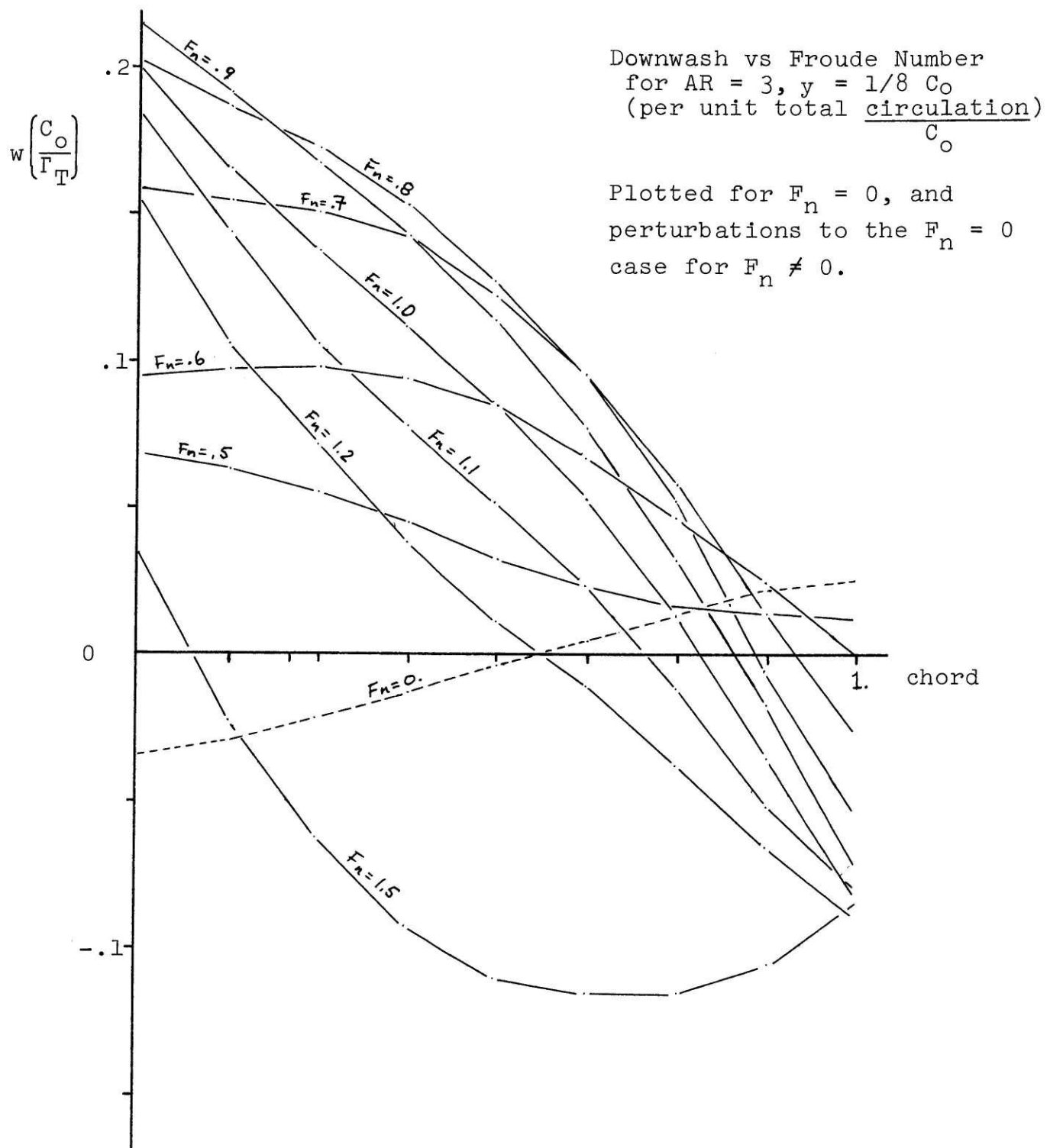


Figure 5 Downwash for elliptical spanwise and chordwise loading

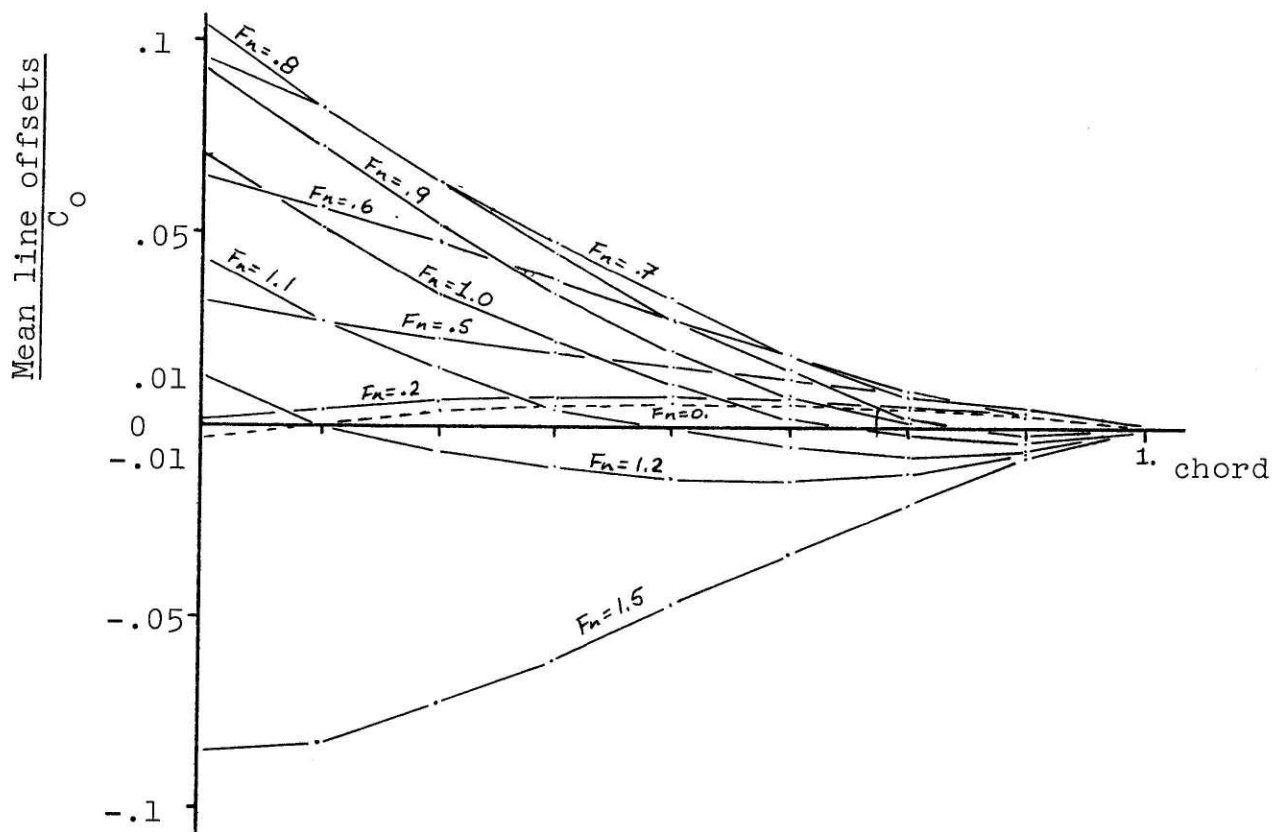


Figure 6 Mean line for elliptical spanwise
and chordwise loading
(Conditions identical to those for Figure 5)

Downwash vs Froude number for
 $AR = 3, y = 1/8 C_o$
 (per unit total circulation)
 C_o

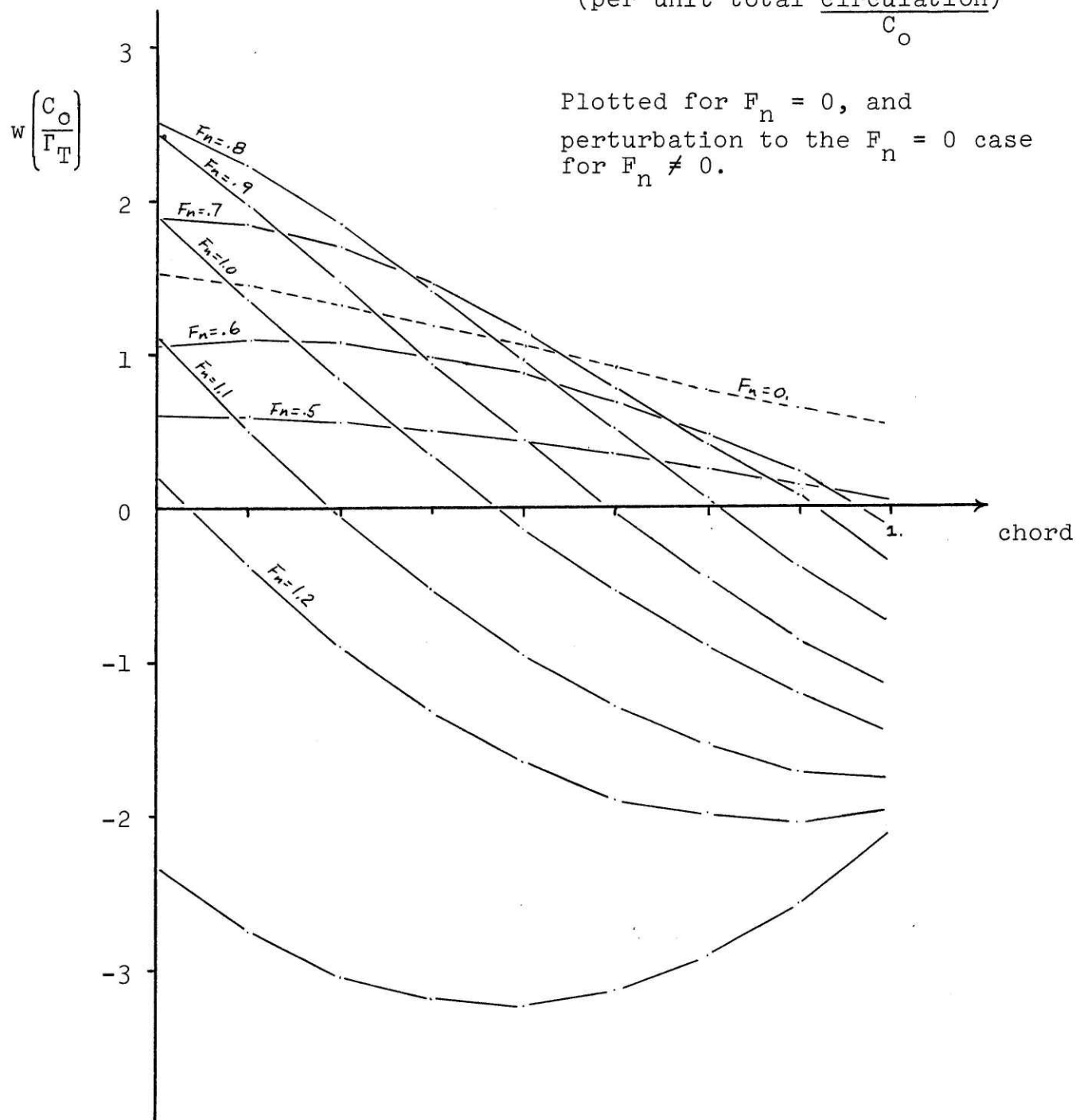


Figure 7 Downwash for cubic spanwise and elliptical chordwise loading

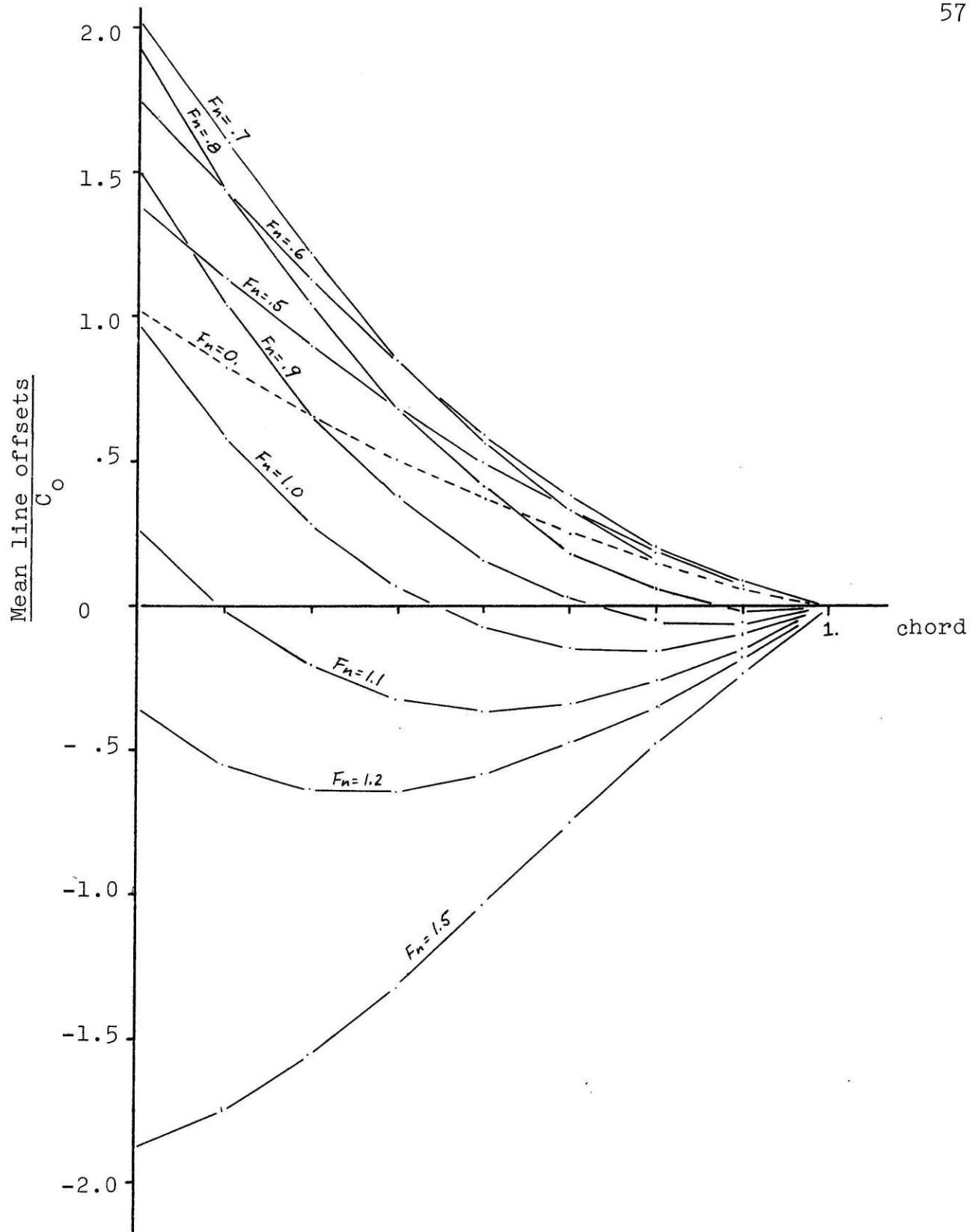


Figure 8 Mean line for cubic spanwise and elliptical chordwise loading
(Conditions identical to those for Figure 7)

appears that larger magnitude wave effects result from the less smooth spanwise loading and the consequential variations in the strength of the free and trailing vortex systems. Because of the significantly larger velocities induced by this second mode, it appears that its strength would be less than the first mode's in any superposition scheme, and therefore, represent a small variation in the overall dynamics of a foil being studied.

For both loadings, the reversal of the downwash reaches a maximum at a Froude number of 0.8. Considering the ratio of the foil's chord to the length of a plane wave propagating in the direction of the foil at a phase velocity equal to the foil's velocity, it can be shown that a Froude number of 0.8 corresponds to a wavelength equal to four chords.

$$V_p = \sqrt{gL_w/2\pi}$$

$$F_n = U/\sqrt{gC_o}$$

Then $V_p = U$ implies

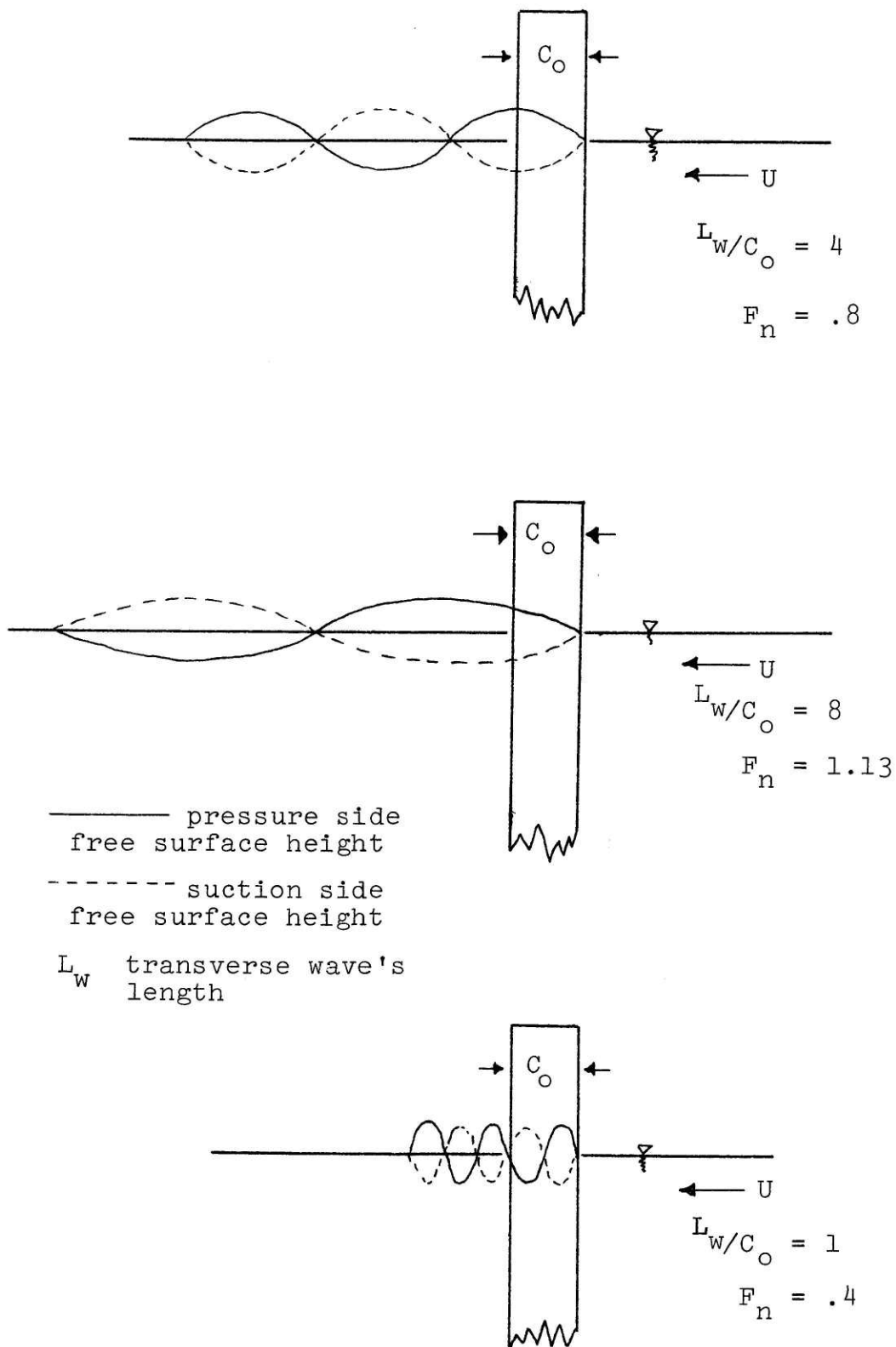
$$L_w/C_o = 2\pi F_n^2$$

where L_w is the length and V_p is the phase velocity of a two dimensional plane progressive wave. For $F_n = 0.8$, $L_w/C_o = 4.02$ as stated above. Recalling that both the streamwise velocity perturbations ϕ_x and the free surface elevation η are equal in magnitude and opposite in sign at adjacent points on the two sides of the foil, a crude physical

explanation for the connection between $L_w/C_o = 4$, and the maximum reversed downwash may be offered. If the wave pattern near the foil is dominated by a transverse wave of length $L_w = 4C_o$ with no elevation jump at the leading edge, there will be a wave crest at the trailing edge on the pressure side and a trough on the suction side. This clearly violates the Kutta condition and the condition requiring continuity of pressure across the wake. One suspects, therefore, that other waves included in the solution cancel this pressure jump at the trailing edge and in the wake. These waves need not be transverse and will, in general, give both streamwise and transverse velocity perturbations. It is these transverse velocities that are suspected of causing the maximum upwash for a Froude number of 0.8. To some extent this effect is anticipated at all Froude numbers, but it will be relatively stronger wherever the transverse wave system has a crest and trough at opposite sides of the trailing edge. Finally, in the $F_n = 0.8$ case, this effect might be expected to reach a maximum since at this Froude number the total side force due to this transverse wave system (per unit wave amplitude) is maximized. At higher Froude numbers the transverse wave's crest is downstream of the foil and at lower Froude numbers the shorter waves on either side will tend to display cancellation effects. Figure 9 illustrates some of these ideas.

The decay of the wave effects below the free surface was investigated in the case of elliptical spanwise and

Figure 9 Idealized transverse wave system of a surface piercing hydrofoil



chordwise loading. Figure 10 illustrates this behavior for depths of $1C_0$, $2C_0$ and $3C_0$ below the surface and generally confirms the anticipated exponential decay below the free surface that is associated with deep water gravity waves.

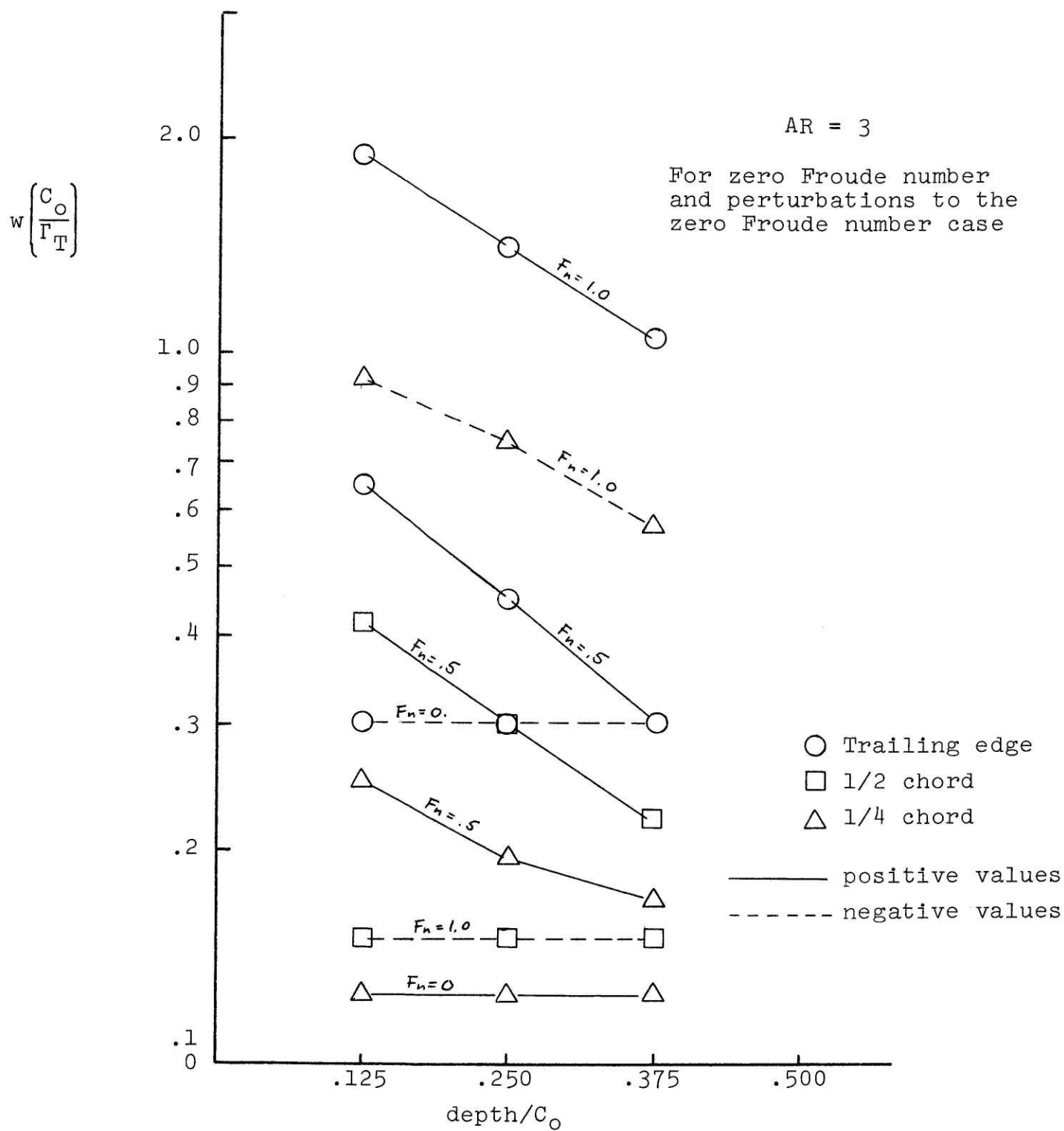


Figure 10 Downwash variation with depth under a free surface for elliptical spanwise and chordwise loading

XII CONCLUSIONS AND FUTURE DIRECTIONS

Two significant results have been achieved. First, a formulation of the surface piercing hydrofoil problem has been developed to represent a foil of arbitrary shape in terms of a distribution of elemental horseshoe vortex singularities. Conditions sufficient to preclude infinities of the free surface elevation (or perturbation velocities at the free surface) have been determined and a variety of possible loading modes have been given along with information sufficient to determine their satisfaction of these conditions.

The second result is the proposed and demonstrated technique of numerically calculating foil shapes for arbitrary loadings. Using a vortex lattice scheme combined with a numerical calculation of a double improper integral, shapes due to any permissible loading can be determined. It appears that using this technique for determining the side forces acting on a known surface peircing foil shape is possible using linear superposition. To reduce the expense of computing a large number of downwash (shape) modes, the existing routines could possibly be modified to more expeditiously perform the several numerical integrations.

A remaining difficulty with the present theoretical results is the apparent inability of linear theory to account for the frequently observed jump in the height of the

free surface at the trailing edge. A discussion of this matter is undertaken in Appendix E. Extension of the analysis to investigate an "inner" region of the flow near the intersection of the track of the foil and the free surface might prove most rewarding.

In summary, a formulation for surface piercing hydrofoils has been developed and the relation between loading and shape has been investigated in several instances to demonstrate the viability of using this formulation and associated numeric techniques to analyze free surface piercing hydrofoils. Future efforts should be directed on two fronts. First, the physics of the trailing edge free surface jump should be studied in greater detail. Second, direct comparisons between theoretical and experimental results should be made for some Froude number, aspect ratio and simple foil shape to determine the applicability of this linear theory to real physical problems.

BIBLIOGRAPHY

- (1) Newman, J. N., "Derivation of the Integral Equation for a Rectangular Lifting Surface", 1961, unpublished
- (2) Milgram, J. H., "Derivation of the Integral Equation for a Free Surface Piercing Lifting Line", 1968, unpublished
- (3) Faulkner, V. M., "The Calculation of Aerodynamic Loading on Surfaces of any Shape", Aeronautical Research Committee R & M No. 1910, 1943
- (4) Milgram, J. H., "The Design and Construction of Yacht Sails", Masters Thesis, M.I.T., Department of Naval Architecture and Marine Engineering, 1962, Cambridge, U.S.A.
- (5) Glauert, H., The Elements of Aerofoil and Airscrew Theory, University Press, Cambridge, U. K., 1948
- (6) Robinson, A. and Laurmann, J. A., Wing Theory, University Press, Cambridge, 1956
- (7) Seeley, R. T., An Introduction to Fourier Series and Integrals, W. A. Benjamin, Inc., New York, 1966
- (8) Erdelyi, ed., Tables of Integral Transforms, Volume 1, Bateman Manuscript Project, ONR, McGraw-Hill Book Company, Inc., 1954
- (9) Lighthill, M. J., Introduction to Fourier Analysis and Generalized Functions, University Press, Cambridge, U.K. 1964
- (10) Ashley, H. and Landahl, M., Aerodynamics of Wings and Bodies, Addison-Wesley Publishing Company, Reading, Massachusetts, 1965
- (11) Copson, E. T., Asymptotic Expansions, Cambridge Tracts in Mathematics and Mathematical Physics, University Press, Cambridge, U. K., 1965
- (12) Newman, J. N., Marine Hydrodynamics, Department of Naval Architecture and Marine Engineering, M.I.T., Cambridge, U.S.A., 1969

- (13) Abramowitz, M. (ed.) and Stegun, I. A. (ed.), Handbook of Mathematical Functions, National Bureau of Standards, Applied Mathematics Series 55, U. S. Government Printing Office, Washington, D. C., 1964
- (14) Prandtl, L. and Tietjens, O. G., Fundamentals of Hydro- and Aeromechanics, Dover Publications, New York, 1957 (copyright United Engineering Trustees, 1934)
- (15) Prandtl, L. and Tietjens, O. G., Applied Hydro- and Aeromechanics, Dover Publications, New York, 1957 (copyright United Engineering Trustees, 1934)
- (16) Van Dyke, M., Perturbation Methods in Fluid Mechanics, Academic Press, New York, 1964
- (17) Letcher, J. S., Transverse Hydrodynamic Forces on Slender Bodies in Free Surface Flows at Low Speed, Ph.D. Thesis, California Institute of Technology, Pasadena, California, 1966
- (18) Peters, A. S. and Stoker, J. J., "The Motion of a Ship As a Floating Rigid Body, in a Seaway", Communications on Pure and Applied Mathematics, Vol. X, pp. 399-490, 1957
- (19) Wehausen, J. V. and Laitone, E. V., "Surface Waves", Handbucher Physik, Band IX, Springer Verlag, Berlin
- (20) Michell, J. H., The Wave-Resistance of a Ship, Phil. Mag., Vol. 45, No. 106, 1898
- (21) Betz, A. and Petersohn, E., "Zur Theorie der Querruder", Zeitschrift fur Angewandte Mathematik und Mechanik (ZAMM), Band 8, Heft 4, August, 1928
- (22) Daoud, N., "Forces and Moments on Asymmetric Yawed Bodies in a Free Surface", Doctoral Thesis, University of California, Berkeley, 1973
- (23) Van Den Brug, J. B., Beukelman, W., Prins, G. J., Hydrodynamic Forces on a Surface Piercing Flat Plate, Report NR 325, Shipbuilding Laboratory, Delft University of Technology, Delft, The Netherlands, 1971
- (24) Ismail, K.A.R., "The Hydrodynamic Theory of Vertical Swept Hydrofoils near a Free Surface and Comparison with Measurement", Doctoral thesis, University of Southampton, Southampton (U.K.), 1972

Appendix A

TRANSFORMATION FROM THE DIPOLE TO
HORSESHOE VORTEX FORMULATION

As given in equation 3.10, the dipole formulation is:

$$\omega(x,y) = -\frac{1}{2\pi C_0} \int_{-\infty}^{\infty} \int_{-\infty}^{\infty} \Gamma(x_0, y_0) \left. \frac{\partial \phi_d}{\partial z} \right|_{z=0} dx_0 dy_0 \quad (A.1)$$

$$\left. \frac{\partial \phi_d}{\partial z} \right|_{z=0} = \frac{1}{r^3} + \frac{1}{r'^3} - \frac{4}{\pi} \operatorname{Re} \int_0^{\frac{\pi}{2}} \int_0^{\infty} \frac{\kappa^3 F^3 \sin^2 \theta}{\kappa - \sec^2 \theta} e^{-\kappa F [y+y_0 + i(x-x_0) \cos \theta]} d\kappa d\theta \quad (A.2)$$

The development for the algebraic terms in the Green's function A.2, is identical to that for classical lifting surface theory and is carried out by returning to the form of the potential with the differentiation, with respect to z_0 , and the limit as z_0 tends to zero taken outside the integrals over x_0 and y_0 . In this form, an integration by parts is performed in the x_0 coordinate leaving an evaluated portion and an integral equation for unknown, $\partial \Gamma / \partial x_0$, which is the negative of the local bound vortex strength, $\gamma(x_0, y_0)$. The steps may be found in many texts including Ashley and Landahl (10).

The double integral contribution may be evaluated by integrating with respect to x_0 inside the κ and θ integrals.

The x_0 integration from equation 3.10 is:

$$I = \int_{-\infty}^1 \Gamma(x_0, y_0) e^{i K F x_0 \cos \theta} dx_0 \quad (A.3)$$

$$I = \frac{\Gamma(x_0, y_0) e^{i K F x_0 \cos \theta}}{i K F \cos \theta} \Big|_{-\infty}^1 + i \int_0^1 \frac{\partial \Gamma}{\partial x_0} \frac{e^{i K F x_0 \cos \theta}}{K F \cos \theta} dx_0 \quad (A.4)$$

The evaluated portion is zero at $x_0 = 1$, because $\Gamma(1, y_0) = 0$ (no load ahead of the leading edge) and as $x_0 \rightarrow -\infty$, when subsequently integrated over the wave number K , the expression with $x_0 \rightarrow -\infty$ will make no contribution due to its highly oscillatory integrand, as is formally demonstrable using the Reimann-Lesbeque Lemma. Again reversing the order of integration, the double integral contribution is:

$$\frac{4}{\pi} \operatorname{Im} \int_0^{\frac{\pi}{2}} \int_0^{\infty} \frac{K^2 F^2 \tan \theta}{K - \sec^2 \theta} \sin \theta \cdot e^{-K F [y + y_0 + i(x - x_0) \cos \theta]} dk d\theta \quad (A.5)$$

The complete expression for $w(x, y)$ in terms of $\gamma(x_0, y_0)$ is given as equation 4.2. Owing to the sign convention $\gamma(x_0, y_0) = -\partial \Gamma / \partial x_0$, a sign change is introduced with the substitution.

Appendix B

TRANSFORMATION FROM HORSESHOE VORTEX TO
NEWMAN'S AND ROBINSON AND LAURMANN'S FORM

As in Appendix A, only the double integral term is treated. Development of the algebraic terms can be found in Robinson and Laurmann (6).

Taking the y_0 integration inside the κ and θ integrals,

$$\begin{aligned}
 I &= \int_0^{AR} \gamma(x_0, y_0) e^{-KFy_0} dy_0 \\
 &= - \left. \frac{\gamma(x_0, y_0) e^{-KFy_0}}{KF} \right|_0^{AR} + \int_0^{AR} \frac{e^{-KFy_0}}{KF} \frac{\partial \gamma}{\partial y_0} dy_0 \\
 &= \frac{\gamma(x_0, 0)}{KF} + \int_0^{AR} \frac{e^{-KFy_0}}{KF} \frac{\partial \gamma}{\partial y_0} dy_0 \\
 &= \frac{1}{KF} \int_0^{AR} \frac{\partial \gamma}{\partial y_0} \left(e^{-KFy_0} - 1 \right) dy_0 \quad (B.1)
 \end{aligned}$$

Returning to a form with the y_0 integration carried out after the κ and θ integrals, the complete formulation is:

$$\begin{aligned}
 \omega(x, y) &= - \frac{1}{2\pi c_0} \int_0^1 \int_0^{AR} \frac{\partial \gamma(x_0, y_0)}{\partial y_0} \left\{ \frac{\sqrt{(x-x_0)^2 + (y-y_0)^2}}{(x-x_0)(y-y_0)} \right. \\
 &\quad \left. - \frac{1}{y-y_0} - \frac{\sqrt{(x-x_0)^2 + (y+y_0)^2}}{(x-x_0)(y+y_0)^2} + \frac{1}{y+y_0} \right.
 \end{aligned}$$

$$-\frac{4}{\pi} \operatorname{Im} \int_0^{\frac{\pi}{2}} \int_0^{\infty} \frac{kF}{k - \sec^2 \theta} \sin \theta \tan \theta \cdot$$

$$e^{-kF(y + i(x-x_0) \cos \theta)} (e^{-kFy_0} - 1) dk d\theta \Big\} dx_0 dy_0$$

(B.2)

Appendix C

THE INFINITE FROUDE NUMBER LIMIT OF THE DOUBLE INTEGRAL TERM IN THE HORSESHOE VORTEX KERNEL

Letting $\lambda = KF$, the double integral term in the horseshoe vortex kernel may be written:

$$I = -\frac{4}{\pi} \operatorname{Im} \int_0^{\frac{\pi}{2}} \int_0^{\infty} \frac{\lambda^2 \tan \theta \sin \theta}{\lambda - F \sec^2 \theta} e^{-\lambda [y+y_0 + i(x-x_0) \cos \theta]} d\lambda d\theta \quad (C.1)$$

Assuming for the moment that the proper interpretation of C.1, as $F \rightarrow 0$ can be made setting $F = 0$,

$$I = -\frac{4}{\pi} \operatorname{Im} \int_0^{\frac{\pi}{2}} \int_0^{\infty} \lambda \tan \theta \sin \theta e^{-\lambda [y+y_0 + i(x-x_0) \cos \theta]} d\lambda d\theta \quad (C.2)$$

Defining $y + y_0 = a$, $x - x_0 = b$;

$$\begin{aligned} I &= +\frac{4}{\pi} \int_0^{\frac{\pi}{2}} \sin \theta \tan \theta \int_0^{\infty} \lambda \sin (\lambda b \cos \theta) e^{-\lambda a} d\lambda d\theta \\ &= +\frac{4}{\pi} \int_0^{\frac{\pi}{2}} \sin \theta \tan \theta \frac{2ab \cos \theta}{[a^2 + b^2 \cos^2 \theta]^2} d\theta \\ &= +\frac{8ab}{\pi} \int_0^{\frac{\pi}{2}} \frac{\sin^2 \theta}{[a^2 + b^2 \cos^2 \theta]^2} d\theta \end{aligned}$$

$$I = \frac{4ab}{\pi} \int_{-\frac{\pi}{2}}^{\frac{\pi}{2}} \frac{\sin^2 \theta}{[a^2 + b^2 \cos^2 \theta]^2} d\theta$$

letting $\xi = \tan \theta$, $d\xi = \sec^2 \theta d\theta$

$$\begin{aligned} I &= \frac{4ab}{\pi} \int_{-\infty}^{\infty} \frac{\xi^2}{\xi^2 + 1} \frac{1}{[a^2 + b^2 \frac{1}{\xi^2 + 1}]^2} \frac{d\xi}{\xi^2 + 1} \\ &= \frac{4ab}{\pi} \frac{1}{a^4} \int_{-\infty}^{\infty} \frac{\xi^2}{[\xi^2 + 1 + b^2/a^2]^2} d\xi \end{aligned}$$

letting $c^2 = 1 + b^2/a^2$

$$I = \frac{4b}{\pi a^3} \int_{-\infty}^{\infty} \frac{\xi^2}{[\xi^2 + c^2]^2} d\xi$$

$$I = \frac{4b}{\pi a^3} \int_{-\infty}^{\infty} \frac{\xi^2}{[\xi + ic]^2 [\xi - ic]^2} d\xi \quad (C.3)$$

This may be evaluated using residue theory. The residue at $\zeta = ic$, is found by expanding $\zeta^2/[\zeta+ic]^2$ about $\zeta = ic$, giving:

$$\frac{\xi^2}{[\xi+ic]^2} = \frac{1}{4} + (\xi-ic) \cdot \frac{-i}{4c} + \dots$$

The residue is then $-\frac{i}{4c}$, the coefficient of the first order pole of the Laurant expansion for the entire integrand.

The integral may then be evaluated.

$$\begin{aligned} I &= \frac{4b}{\pi a^3} \cdot 2\pi i \cdot \left(-\frac{i}{4c}\right) \\ &= \frac{2(x-x_0)}{(y+y_0)^2 \sqrt{(x-x_0)^2 + (y+y_0)^2}} \quad (C.4) \end{aligned}$$

which is the proper result for the bound vorticity, but doesn't include the effect of the trailing vorticity in the wake. This might have been anticipated since the partial integration carried out in the wake in arriving at the horse-shoe formulation is invalid for the case $F = 0$. From equation A.4, with the negative infinite limit replaced by $-B$,

$$\lim_{B \rightarrow -\infty} - \frac{\Gamma(B, y_0) e^{iKF B \cos \theta}}{iKF \cos \theta} \quad (C.5)$$

Noting that for a unit horseshoe $-\Gamma(+B, y_0) \rightarrow -1$ as $B \rightarrow -\infty$ and reintroducing C.5 into the double integral A.2,

$$\lim_{B \rightarrow -\infty} \frac{4}{\pi} \operatorname{Re} \int_0^{\frac{\pi}{2}} \int_0^{\infty} \frac{(KF)^3 \sin^2 \theta}{k - \sec^2 \theta} \frac{1}{iKF \cos \theta} e^{-KF[y+y_0+i(x-B)\cos\theta]} dk d\theta$$

$$\lim_{B \rightarrow -\infty} \frac{4}{\pi} \operatorname{Im} \int_0^{\frac{\pi}{2}} \int_0^{\infty} \frac{(KF)^2}{k - \sec^2 \theta} \sin \theta \tan \theta e^{-KF[y+y_0+i(x-B)\cos\theta]} dk d\theta$$

Again, letting $\lambda = KF$, this is identical, except for sign, to the integral in C.1, and the result may be written directly.

$$\lim_{B \rightarrow -\infty} -\frac{2(x-B)}{(y+y_0)^2} \frac{1}{\sqrt{(x-B)^2 + (y+y_0)^2}} = -\frac{2}{(y+y_0)^2} \quad (C.7)$$

Thus, in the limit as $F \rightarrow 0$, the double integral term gives

$$-\frac{2}{(y+y_0)^2} + \frac{2(x-x_0)}{(y+y_0)^2 \sqrt{(x-x_0)^2 + (y+y_0)^2}} \quad (C.8)$$

and, in effect, transforms the Green's function into that which satisfies $\phi = 0$ on $y = 0$, the infinite Froude number limit of the free surface boundary condition.

Appendix D

VERTICAL LOAD RESTRICTIONS FOR LIFTING LINES

For small $(y \pm y_0)$, the poles in the kernel of equation 7.6 dominate the logarithmic singularity. Thus, for small $(y \pm y_0)$

$$\omega(o, y) \approx \frac{1}{2\pi c_0} \int_0^\epsilon \Gamma'(y_0) \left[\frac{1}{(y-y_0)^2} - \frac{1}{(y+y_0)^2} \right] dy_0 \quad (D.1)$$

where ϵ has been chosen such that the approximation is valid for $0 < y_0 < \epsilon$. Returning to the form preceding differentiation of the potential with respect to z and taking the limit of z tends to zero,

$$\omega(o, y) = \lim_{z \rightarrow 0} \frac{\partial}{\partial z} \frac{1}{2\pi c_0} \int_0^\epsilon \Gamma'(y_0) \left\{ \frac{z}{(y-y_0)^2 - z^2} - \frac{z}{(y+y_0)^2 - z^2} \right\} dy_0 \quad (D.2)$$

Integrating D.2 twice by parts and taking the limit $z \rightarrow 0$ and derivative with respect to z

$$\omega(o, y) = \frac{-1}{2\pi c_0} \left\{ \Gamma'(\epsilon) \frac{2y}{\epsilon^2 - y^2} + \frac{1}{2} \frac{\partial \Gamma(\epsilon)}{\partial y_0} \ln \left(\frac{\epsilon + y}{\epsilon - y} \right) + \frac{2}{y} \Gamma(o) + \frac{\pi}{2} \left(y \frac{\partial \Gamma(\epsilon)}{\partial y_0} - \Gamma(y) - \lim_{q \rightarrow 0} q \frac{\partial \Gamma(q)}{\partial q} \right) \right\} \quad (D.3)$$

For $w(0,y)$ to remain bounded as $y \rightarrow 0$, the term $\frac{2}{y} \Gamma(0)$ requires $\Gamma(0) = 0$, and the term

$$\lim_{q \rightarrow 0} q \frac{\delta \Gamma(q)}{\delta q} \quad (\text{D.4})$$

requires that $\Gamma(q)$ tend to zero at least as fast as $q \ln q$ as $q \rightarrow 0$.

Appendix E

FREE SURFACE ELEVATION DISCONTINUITIES

A frequently observed phenomenon is a jump in the elevation of the free surface at the trailing edge of a surface piercing foil. Although this effect appears to be of first order magnitude (crude experiments indicate a linear relation between angle of attack and this elevation jump), it has not been possible to predict it as part of the solution to the linearized problem.

The difficulty arises from the imposition of the pressure continuity condition across the wake. Without a free surface (at zero Froude number), the pressure everywhere in the flow is given by the linearized Bernoulli equation:

$$p = +\rho U \phi_x \quad , \quad y > 0 \quad (E.1)$$

This relation also applies at points below a free surface, but does not hold on the free surface where the linearized dynamic free surface boundary condition gives:

$$p = +\rho U \phi_x - \rho g \eta \quad , \quad \text{on } y = 0 \quad (E.2)$$

and permits an elevation jump while maintaining the imposed pressure continuity providing there is a corresponding discontinuity in the streamwise velocity perturbation, ϕ_x .

Although a plausible explanation for the free surface elevation jump can be argued, based on line singularities

of presently unknown form and strength, to do so without first thoroughly investigating a possible inner region of the flow at the intersection of the free surface and the foil would be pure conjecture. It should also be noted that equally plausible nonlinear effects can be argued as the mechanism producing the free surface jump.

Appendix F

CONVERSION BETWEEN FORMS OF THE FREE SURFACE SOURCE POTENTIAL

The familiar expression,

$$\frac{1}{r} = \frac{1}{(x^2 + y^2 + z^2)^{1/2}} = \frac{1}{2\pi} \int_0^\infty dk \int_{-\pi}^{\pi} d\theta \left\{ \begin{array}{l} e^{-ky} \\ e^{ik(x \cos \theta + z \sin \theta)} \end{array} \right\} \quad (\text{F.1})$$

may be reduced to:

$$\frac{1}{r} = \frac{2}{\pi} \int_0^{\frac{\pi}{2}} d\theta \int_0^\infty dk e^{-ky} \cos(\kappa z \sin \theta) \cos(\kappa x \cos \theta) \quad (\text{F.2})$$

From Wehausen (19)(equation 13.36), using our coordinates, the source potential is:

$$\phi_s = \frac{1}{r} - \frac{1}{r'} - \frac{4\gamma}{\pi} \int_0^{\frac{\pi}{2}} d\theta \int_0^\infty \frac{e^{-\lambda(y+y_0)}}{\lambda \cos^2 \theta - \gamma} \cos[\lambda(z-z_0) \sin \theta] \cos[\lambda(x-x_0) \cos \theta] d\lambda d\theta \quad (\text{F.3})$$

adding and subtracting $2/r'$ in its two forms,

$$\phi_s = \frac{1}{r} + \frac{1}{r'} - \frac{4}{\pi} \int_0^{\frac{\pi}{2}} \int_0^{\infty} \left[\frac{\nu}{\lambda \cos^2 \theta - \nu} + 1 \right] e^{-\lambda(y+y_0)} \cos(\lambda(z-z_0) \sin \theta) \cos(\lambda(x-x_0) \cos \theta) d\lambda d\theta \quad (\text{F.4})$$

which reduces to the form stated in equation 3.3,

$$\phi_s = \frac{1}{r} + \frac{1}{r'} - \frac{4}{\pi} \operatorname{Re} \int_0^{\frac{\pi}{2}} \int_0^{\infty} \frac{\lambda}{\lambda - \nu \sec^2 \theta} \cos[\lambda(z-z_0) \sin \theta] e^{-\lambda[y+y_0+i(x-x_0) \cos \theta]} d\lambda d\theta \quad (\text{F.5})$$

Appendix G

WAVE EFFECTS OF THE HORSESHOE VORTEX SINGULARITY

At one stage in the development of the present formulation, it was believed that the downwash contributed by the double integral term of the horseshoe vortex kernel (equation 4.2) could be tabulated as a function of $(x - x_0, y + y_0, F)$ and used in computing the downwashes corresponding to various loadings. This approach, however, improperly restricted the permitted loadings near the free surface (zero loading at the surface) and was abandoned.

One aspect of this work is significant, and this is the relation between the forms of the various terms in the horseshoe vortex kernel. Figure 10 shows the downwash contributed by the double integral term of the kernel for various finite values of the parameter, v , and the limiting case $v = 0$. It can be seen that the downwash tends toward the proper limit quite rapidly upstream and less so downstream where anticipated radiating waves give an oscillatory downwash.

Figure 11 shows the effect of approaching the free surface, and the resulting increases in the downwash which are seen to be singular roughly as $1/(y+y_0)^2$ as $(y+y_0) \rightarrow 0$. Again this result might have been anticipated as this is the manner in which the other terms in the kernel behave for $(y-y_0) \rightarrow 0$ and $(y+y_0) \rightarrow 0$, respectively.

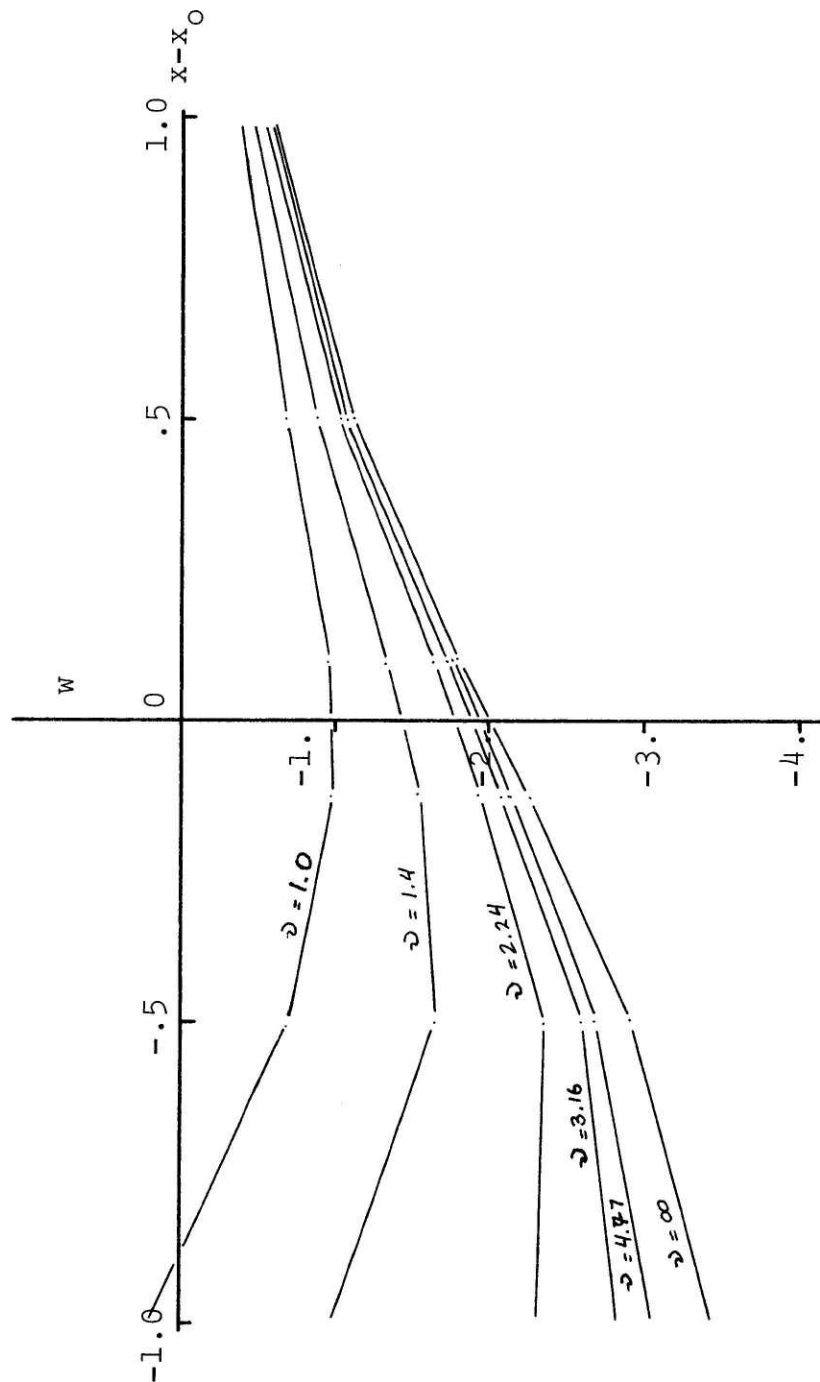
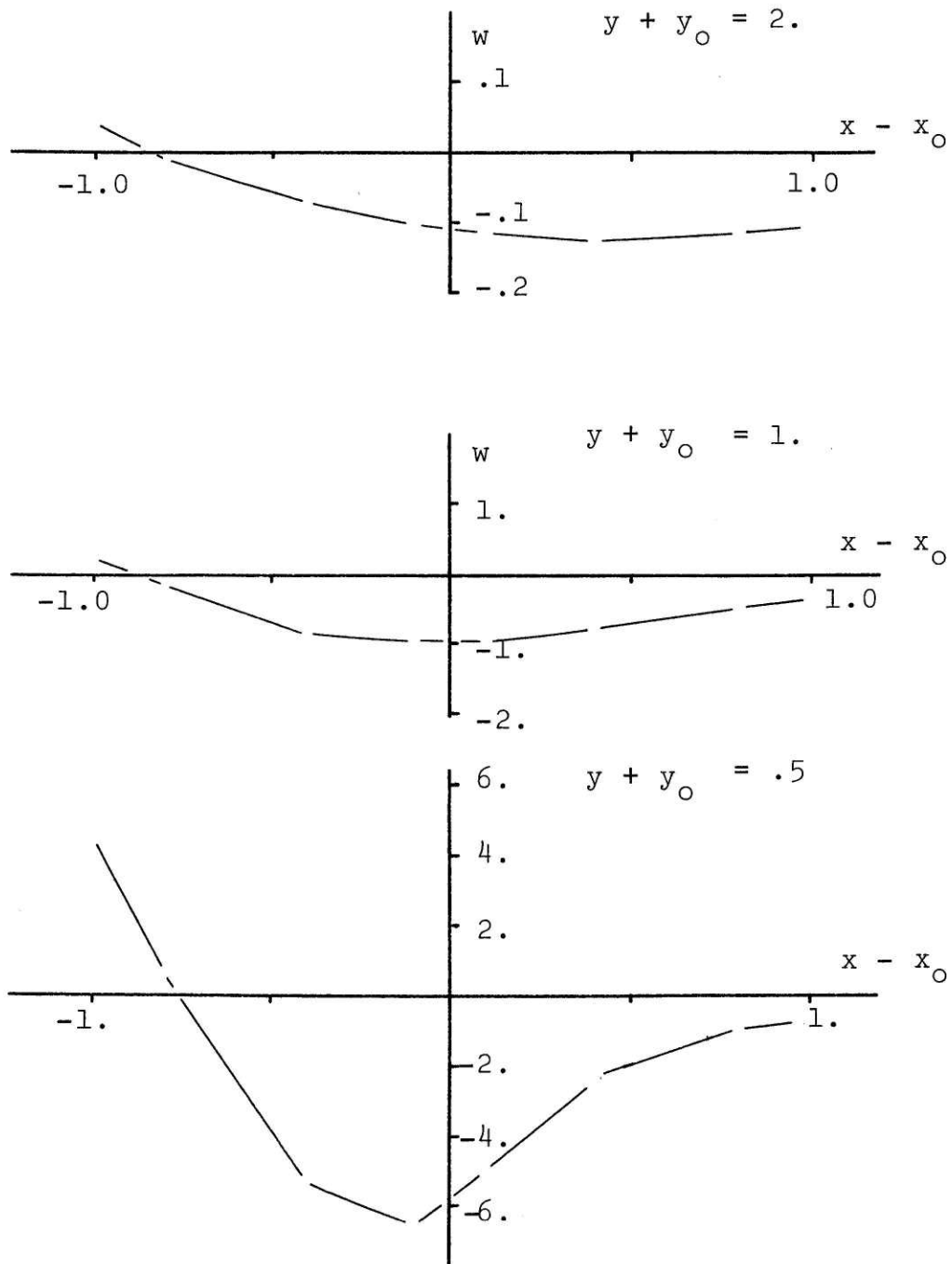


Figure 11 Point horseshoe vortex singularity: downwash versus $(x - x_0)$ for various Froude numbers* at fixed $y + y_0 = 1$.
 (*) In this case, the dimensional parameter v

Figure 12 Point horseshoe vortex singularity: downwash versus $(x - x_0)$ for varying $(y + y_0)$ at fixed $v = 1$.



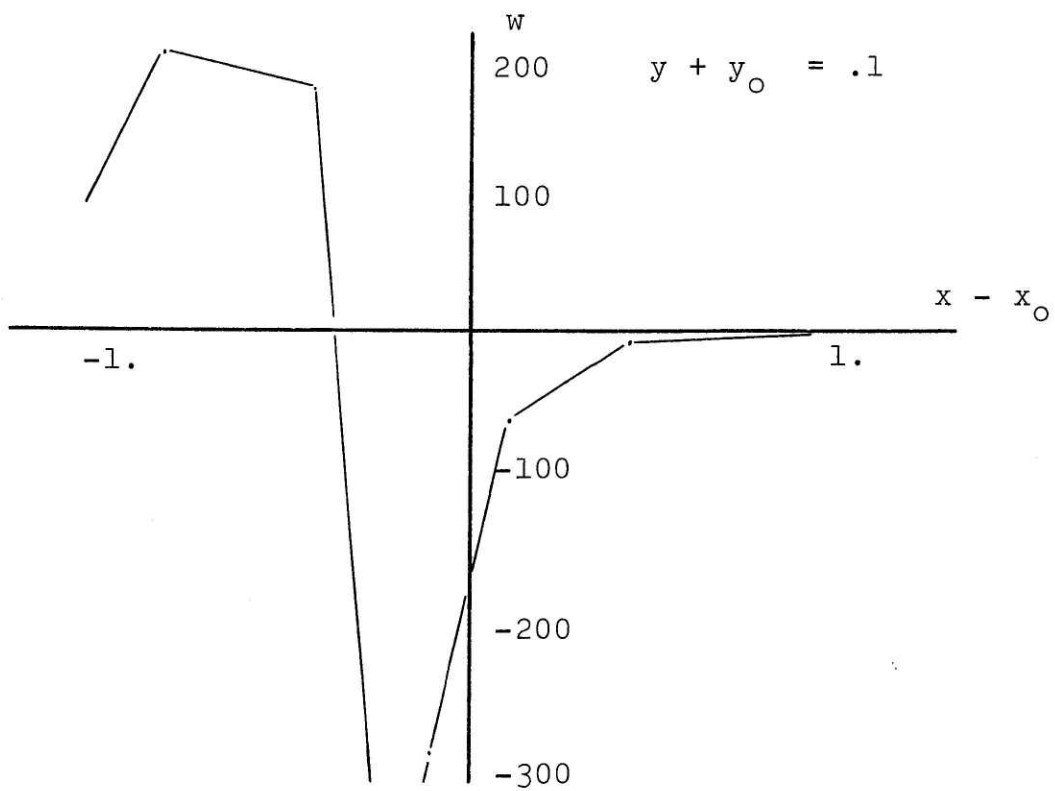
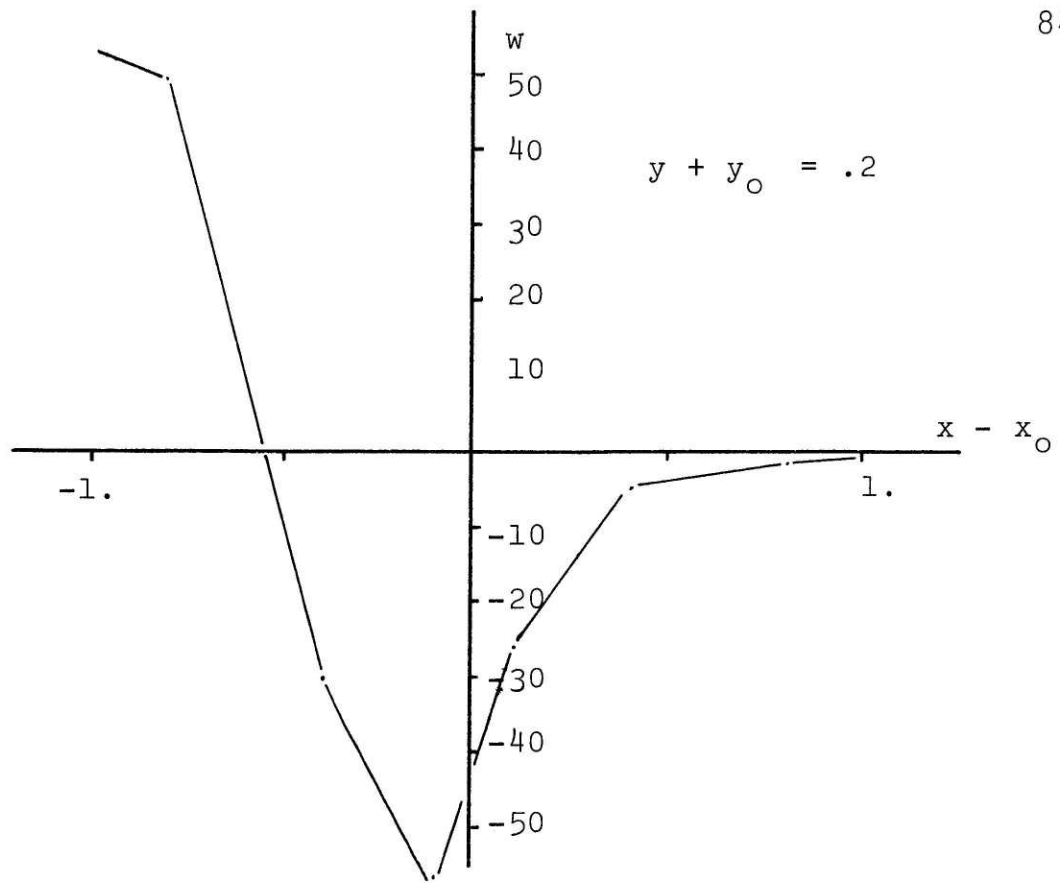


Figure 12
(continued)

Appendix H

LISTINGS OF COMPUTER PROGRAMS USED TO EVALUATE DISTRIBUTED
LOAD DOWNWASH CONTRIBUTIONS FROM THE DOUBLE INTEGRAL IN
THE HORSESHOE VORTEX KERNEL USING LOADING TRANSFORMS

C	MAIN PROGRAM FOR CALCULATING DOWNWASH THRU LOAD TRANSFORMS	MAINCC01
	COMMON ER	MAINCC02
	DIMENSION W(10)	MAINCC03
	DATA IR,IW/5,6/	MAINCC04
1	FORMAT(8F10.5)	MAINCC05
2	FORMAT('1DOWNWASH ALONG CHORD FOR UNIT CIRCULATION:')	MAINCC06
3	FORMAT('0ASPECT RATIO:',F10.5)	MAINCC07
4	FORMAT('0FROUDE NUMBER:',F10.5)	MAINCC08
5	FORMAT('0CHORD:',F10.5)	MAINCC09
6	FORMAT('0FREE STREAM:',F10.5)	MAINCC10
7	FORMAT(1H ,10E11.3)	MAINCC11
8	FORMAT(1H1)	MAINCC12
9	FORMAT('0DOWNWASH WITH LEADING EDGE AT RIGHT:',//)	MAINCC13
11	FORMAT('0DEPTH:',F10.5)	MAINCC14
	READ(IR,1) CHD,AR,ER	MAINCC15
10	READ(IR,1) Y,F	MAINCC16
	IF(Y.LT.0.0) GOTO 40	MAINCC17
	UINF=SQRT(32.2*CHD/F)	MAINCC18
	DO 100 I=1,9	MAINCC19
	X=.125*FLOAT(I-1)	MAINCC20
	WRITE(IW,1) X,Y,F,CHD,AR,ER	MAINCC21
	CALL WAVES(X,Y,F,CHD,AR,ANS)	MAINCC22
100	W(I)=ANS	MAINCC23
	WRITE(IW,2)	MAINCC24
	F=SQRT(1./F)	MAINCC25
	WRITE(IW,3) AR	MAINCC26
	WRITE(IW,4) F	MAINCC27
	WRITE(IW,5) CHD	MAINCC28
	WRITE(IW,6) UINF	MAINCC29
	WRITE(IW,11) Y	MAINCC30
	WRITE(IW,9)	MAINCC31
	WRITE(IW,7) (W(I),I=1,9)	MAINCC32
	WRITE(IW,8)	MAINCC33
	GOTO 10	MAINCC34
40	STOP	MAINCC35
	END	MAINCC36

```

SUBROUTINE WAVES(X,Y,F,CHD,AR,ANS)
COMMON ER
DIMENSION Q(1000)
DATA PI/3.14159/
DATA IR,IW/5,6/
IER=0
IB=2
IE=10
IS=1
NI=10
PANS=10
Q(1)=0.0
80 H=1./FLCAT(NI)
Q(NI+1)=0.0
DO 100 I=IB,IE,IS
D3=H*(I-1)
TH=PI*(D3**2)/2.
P=SIN(TH)
CALL WVNBR(P,F,AR,X,Y,ANS,IER)
IF(IER.NE.0) GOTO 200
CALL GAMMA(F/(P**2),P,AR,GAMR,GAMI)
R1=F*X/P
R2=GAMR*COS(R1)+GAMI*SIN(R1)
IF(R2.EQ.0.0) GOTO 90
R=-F*Y/(P**2)+ALCG(ABS(PI*R2))
IF(R+180.) 90,90,91
90 R=0.0
GOTO 100
91 R=(R2/ABS(R2))*EXP(R)
100 Q(I)=(1.-P**2)*(ANS+R)*PI*D3
CALL SIMR(IE,H,Q,ANS)
TEST=ABS((ANS-PANS)/ANS)
IF(TEST.LT.ER) GOTO 150
IF(IE.GT.499) GOTO 140
CALL SPRD(Q,NI+1)
NI=NI*2

```

```

WAVEC001
WAVEC002
WAVEC003
WAVEC004
WAVEC005
WAVEC006
WAVEC007
WAVEC008
WAVEC009
WAVEC010
WAVEC011
WAVEC012
WAVEC013
WAVEC014
WAVEC015
WAVEC016
WAVEC017
WAVEC018
WAVEC019
WAVEC020
WAVEC021
WAVEC022
WAVEC023
WAVEC024
WAVEC025
WAVEC026
WAVEC027
WAVEC028
WAVEC029
WAVEC030
WAVEC031
WAVEC032
WAVEC033
WAVEC034
WAVEC035
WAVEC036

```

```

        IE=NI
        IS=2
        PANS=ANS
        GOTO 80
140    WRITE(IW,1) X,Y,F,CHD,AR,ANS,TEST
1      FORMAT(' WAVES:',7E12.3)
        WRITE(IW,4)
4      FORMAT(' WAVES NOT CONVERGENT')
150    ANS=ANS*(-2./(CHD*(PI**2)))
        WRITE(IW,1) ANS
        J=NI+1
        WRITE(IW,3) (Q(I),I=1,J)
        RETURN
200    WRITE(IW,2) IER,ANS
2      FORMAT(' WVNBR NOT CONVERGENT',I10,E20.6)
        J=NI+1
        WRITE(IW,3) (Q(I),I=1,J)
3      FORMAT(1H ,10E11.3)
        STOP
        END
        SUBROUTINE SPRC(S,N)
        DIMENSION S(1)
        NN=N-1
        DO 10 I=1,NN
        J=N-I+1
        K=2*J-1
10     S(K)=S(J)
        RETURN
        END

```

```

WAVEC037
WAVEC038
WAVEC039
WAVEC040
WAVEC041
WAVEC042
WAVEC043
WAVEC044
WAVEC045
WAVEC046
WAVEC047
WAVEC048
WAVEC049
WAVEC050
WAVEC051
WAVEC052
WAVEC053
WAVEC054
WAVEC055
WAVEC056
WAVEC057
WAVEC058
WAVEC059
WAVEC060
WAVEC061
WAVEC062
WAVEC063
WAVEC064
WAVEC065

```



```
SUBROUTINE TRAP(NI,H,F,ANS)
DIMENSION F(1)
ANS=0.0
IF(NI.EQ.0) GOTO 20
ANS=(F(1)+F(NI+1))*C.5
DO 10 I=2,NI
10  ANS=ANS+F(I)
   ANS=ANS*H
20  RETURN
END
```

```
TRAP0001
TRAP0002
TRAP0003
TRAP0004
TRAP0005
TRAP0006
TRAP0007
TRAP0008
TRAP0009
TRAP0010
```

C SUBROUTINE FREQ(P,X,AR,A)
 A=P*(2.-X)
 MAXIMUM RADIAN FREQUENCY OF INTEGRANDS SINUSOIDS
 RETURN
 END

FRECC001
FRECC002
FRECC003
FRECC004
FRECC005

```
      SUBROUTINE SIMR(NI,H,FUNC,ANS)
      DIMENSION FUNC(1)
      K=NI+1
      ANS=FUNC(1)+FUNC(K)
10     DO 10 J=2,NI,2
      ANS=ANS+4*FUNC(J)
      IF(NI.EQ.2)GOTO 30
      K=NI-1
20     DO 20 J=3,K,2
      ANS=ANS+2*FUNC(J)
30     ANS=ANS*H/3.
      RETURN
      END
```

```
SIMRC001
SIMRC002
SIMRC003
SIMRC004
SIMRC005
SIMRC006
SIMRC007
SIMRC008
SIMRC009
SIMRC010
SIMRC011
SIMRC012
SIMRC013
```

	SUBROUTINE WVNBR(P,F,AR,X,Y,TOTAL,IER)	WVNRC001
	COMMON ER	WVNRC002
	DIMENSION F1(5000)	WVNRC003
	DATA IR,IW/5,6/	WVNRC004
	DATA PI/3.14159/	WVNRC005
	T1=0.0	WVNRC006
	T2=0.0	WVNRC007
	T3=0.0	WVNRC008
	IER=0	WVNRC009
	TOTAL=0.0	WVNRC010
	RS=F/(P**2)	WVNRC011
	CALL FREQ(P,X,AR,RADF)	WVNRC012
C	RADF IS MAXIMUM RADIAN FREQUENXY	WVNRC013
C	TEN INTERVALS PER MINIMUM PERIID	WVNRC014
	DR=PI/(5.*RADF)	WVNRC015
	DRX=.25/Y	WVNRC016
	DRS=RS/4.	WVNRC017
	D2=DR	WVNRC018
	IF(D2.GT.DRX) D2=DRX	WVNRC019
	IF(D2.GT.DRS) D2=DRS	WVNRC020
	DR=.2*DR	WVNRC021
	D2=.2*D2	WVNRC022
C	CIW IS CAUCHY INTEGRAL GAP HALF WIDTH	WVNRC023
	CIW=.5*D2	WVNRC024
	IF(CIW.GT..1) CIW=.1	WVNRC025
	UPLS=RS-CIW	WVNRC026
	UPLX=170./Y	WVNRC027
	UPLL=100./AR	WVNRC028
	UL=UPLS	WVNRC029
	IF(UL.GT.UPLL) UL=UPLL	WVNRC030
	IF(UL.GT.UPLX) UL=UPLX	WVNRC031
	NI=UL/D2+1.	WVNRC032
	I=NI/2	WVNRC033
	IF(I*2.NE.NI) NI=NI+1	WVNRC034
	D2=UL/FLCAT(NI)	WVNRC035
C	PORTION CUT THE SINGULARITY	WVNRC036

	F1(1)=0.0	WVNRC037
	DO 100 I=1,NI	WVNRC038
	R=I*D2	WVNRC039
	J=I+1	WVNRC040
	CALL GAMMA(R,P,AR,GAMR,GAMI)	WVNRC041
100	F1(J)=EXP(-Y*R)*(GAMI*COS(R*X*P)-GAMR*SIN(R*X*P))/((P**2)*R-F)	WVNRC042
	CALL TRAP(NI,D2,F1,T1)	WVNRC043
	IF(UL.LT.UPLS) GOTO 300	WVNRC044
C	PRINCIPAL VALUE PART ASSUMING FUNCTION LESS POLE BEHAVES	WVNRC045
C	LINEARLY FROM RS-CIW TO RS+CIW	WVNRC046
	R=RS+CIW	WVNRC047
	CALL GAMMA(R,P,AR,GAMR,GAMI)	WVNRC048
	F1(1)=EXP(-Y*R)*(GAMI*COS(R*X*P)-GAMR*SIN(R*X*P))	WVNRC049
	R=RS-CIW	WVNRC050
	F1(2)=EXP(-Y*R)*(GAMI*COS(R*X*P)-GAMR*SIN(R*X*P))	WVNRC051
	T2=F1(1)-F1(2)	WVNRC052
C	SINGULARITY TO INFINITY	WVNRC053
	TOTAL=T1+T2	WVNRC054
	J=0	WVNRC055
	RL=RS+CIW	WVNRC056
225	DO 250 I=1,16	WVNRC057
	R=RL+(I-1)*DR	WVNRC058
	CALL GAMMA(R,P,AR,GAMR,GAMI)	WVNRC059
250	F1(I)=EXP(-Y*R)*(GAMI*COS(R*X*P)-GAMR*SIN(R*X*P))/((P**2)*R-F)	WVNRC060
	CALL TRAP(15,DR,F1,T3)	WVNRC061
	TEST=ABS(T3/(TOTAL+T3))	WVNRC062
	TOTAL=TOTAL+T3	WVNRC063
	IF(TEST.LT.ER) GOTO 275	WVNRC064
	J=J+1	WVNRC065
	IF(J.GT.60) GOTO 410	WVNRC066
	RL=RL+15.*DR	WVNRC067
	GOTO 225	WVNRC068
275	RETURN	WVNRC069
300	TOTAL=T1	WVNRC070
	RETURN	WVNRC071
400	IER=-NI	WVNRC072

410 TOTAL=R1
RETURN
IER=1
TOTAL=RL
RETURN
END

WVNRC073
WVNRC074
WVNRC075
WVNRC076
WVNRC077
WVNRC078

	SUBROUTINE GAMMA(S,P,AR,GAMR,GAMI)	GAM10001
C	CUBIC SPANWISE AND ELLIPTICAL CHORDWISE LOADING	GAM10002
	DATA IW,IR/5,6/	GAM10003
	DATA PI/3.14159/	GAM10004
	IF(AR*S.GT.100.) GOTO 10	GAM10005
	Z=S*P	GAM10006
	IF(Z.GT..82355E+06) GOTO 10	GAM10007
C	COMPUTE BESSEL FUNCTION OF THE FIRST KIND ORDER ONE USING	GAM10008
C	POLYNOMIAL APPROXIMATION GIVEN IN A AND S HANDBOOK	GAM10009
	IF (Z) 10,10,15	GAM10010
10	R1=C.0	GAM10011
	GAMR=0.0	GAM10012
	GAMI=0.0	GAM10013
	RETURN	GAM10014
15	IF(Z-3.) 16,18,18	GAM10015
16	Z1=Z/3.	GAM10016
	IF(Z1.LT.1.E-09) GOTO 12	GAM10017
	R1=0.5-.56250*(Z1**2)+.21094*(Z1**4)-.03954*(Z1**6)+.00443*(Z1**8)	GAM10018
	GOTO 17	GAM10019
12	R1=0.5	GAM10020
17	R1=R1*Z	GAM10021
	GOTO 20	GAM10022
18	Z1=3./Z	GAM10023
	IF(Z1.LT.1.E-50) GOTO 10	GAM10024
	IF(Z1.LT.1.E-10) GOTO 13	GAM10025
	F1=.79788+.00000156*Z1+.01659667*(Z1**2)+.00017105*(Z1**3)-.002495	GAM10026
	111*(Z1**4)+.00113653*(Z1**5)	GAM10027
	T1=Z-2.35619+.125*Z1+.0000656*(Z1**2)-.00637879*(Z1**3)+.0007435*(GAM10028
	1Z1**4)+.000798*(Z1**5)	GAM10029
	GOTO 19	GAM10030
13	T1=Z	GAM10031
	F1=.79788	GAM10032
19	R1=F1*COS(T1)/SQRT(Z)	GAM10033
20	CONTINUE	GAM10034
	R=S	GAM10035
	R2= (EXP(-AR*R)*((AR**2)/R+4.*AR/(R**2)+6./(R**3))+2.*AR/(R**2)	GAM10036

```
1-6./(R**3)
150  GAMR=24.*R1*R2*COS(S*P)
      GAMI=24.*R1*R2*SIN(S*P)
      RETURN
      END
```

```
GAM10037
GAM10038
GAM10039
GAM10040
GAM10041
```


	SUBROUTINE GAMMA(S,P,AR,GAMR,GAMI)	GAM20001
C	ELLIPITICAL SPANWSIE AND CHORDWISE LOADING	GAM20002
	DIMENSION G(51)	GAM20003
	DATA PI/3.14159/	GAM20004
	DATA IW,IR/5,6/	GAM20005
	DATA G/0.0,.047939,.091990,.132480,.169710,.203952,.235457,.264454	GAM20006
	1,.291151,.315740,.338395,.359276,.378530,.396290,.412679,.427810,.	GAM20007
	2441783,.454694,.466629,.477666,.487877,.497329,.506083,.514194,.52	GAM20008
	31712,.528625,.535156,.541164,.546746,.551933,.556757,.561246,.5654	GAM20009
	426,.569319,.572948,.576333,.579492,.582442,.585199,.587776,.590187	GAM20010
	5,.592445,.594560,.596542,.598402,.600147,.601787,.603328,.604777,.	GAM20011
	6606142,.607426/	GAM20012
	Z=S*P	GAM20013
	IF(Z.GT..82355E+06) GOTO 10	GAM20014
C	COMPUTE BESSEL FUNCTION OF THE FIRST KIND ORDER ONE USING	GAM20015
C	POLYNOMIAL APPROXIMATION GIVEN IN A AND S HANDBOCK	GAM20016
	IF (Z) 10,10,15	GAM20017
10	R1=C.0	GAM20018
	GAMR=0.0	GAM20019
	GAMI=0.0	GAM20020
	RETURN	GAM20021
15	IF(Z-3.) 16,18,18	GAM20022
16	Z1=Z/3.	GAM20023
	IF(Z1.LT.1.E-09) GOTO 12	GAM20024
	R1=C.5-.56250*(Z1**2)+.21094*(Z1**4)-.03954*(Z1**6)+.00443*(Z1**8)	GAM20025
	GOTO 17	GAM20026
12	R1=0.5	GAM20027
17	R1=R1*Z	GAM20028
	GOTO 20	GAM20029
18	Z1=3./Z	GAM20030
	IF(Z1.LT.1.E-50) GOTO 10	GAM20031
	IF(Z1.LT.1.E-10) GOTO 13	GAM20032
	F1=.79788+.00000156*Z1+.01659667*(Z1**2)+.00017105*(Z1**3)-.002495	GAM20033
	111*(Z1**4)+.00113653*(Z1**5)	GAM20034
	T1=Z-2.35619+.125*Z1+.0000656*(Z1**2)-.00637879*(Z1**3)+.0007435*(GAM20035
	1Z1**4)+.000798*(Z1**5)	GAM20036

	GOTO 19	GAM20037
13	T1=Z	GAM20038
	F1=.79788	GAM20039
19	R1=F1*COS(T1)/SGRT(Z)	GAM20040
20	CONTINUE	GAM20041
C	MODIFIED STRUVE FUNCTION LESS MODIFIED BESSEL FUNCTION OF	GAM20042
C	THE SECOND KIND: BOTH ORDER ONE: FROM TABLES FOR SMALL	GAM20043
C	ARGUMENT AND VIA ASYMPTOTIC EXPANSION FOR LARGE	GAM20044
	Z=AR*S	GAM20045
	IF(Z.GT.5.) GOTO 100	GAM20046
	IF(Z.EQ.5.) GOTO 90	GAM20047
	I=10.*Z+1.	GAM20048
	J=I+1	GAM20049
	R2=G(I)+(G(J)-G(I))*(10.*Z-I+1.)	GAM20050
	GOTO 150	GAM20051
90	R2=G(51)	GAM20052
	GOTO 150	GAM20053
100	R2=-1.+1./(Z**2)	GAM20054
	IF(Z.LT.6.93) GOTO 140	GAM20055
	R2=R2+48./(Z**4)+180./(Z**6)	GAM20056
140	R2=-R2*2./PI	GAM20057
150	GAMR=(4./AR)*R1*R2*COS(S*P)	GAM20058
	GAMI=(4./AR)*R1*R2*SIN(S*P)	GAM20059
	RETURN	GAM20060
	END	GAM20061

Appendix I

LISTINGS OF COMPUTER PROGRAMS USED TO EVALUATE
DISTRIBUTED LOAD DOWNWASH CONTRIBUTIONS FROM THE
ZERO FROUDE NUMBER TERMS IN THE HORSESHOE VORTEX KERNEL

C	DOUBLE ASPECT RATIO VORTEX VATTICE PROGRAM	VCRLC001
	DIMENSION SPL(30),CHL(10)	VCRLC002
	DIMENSION W(10)	VCRLC003
	DATA IR,IW/5,6/	VCRLC004
	READ(IR,1) CHD,AR,NC,NS	VCRLC005
1	FORMAT(2F10.5,2I5)	VCRLC006
	WRITE(IW,1) CHD,AR,NC,NS	VCRLC007
C	GIVES DOWNWASH PER UNIT CIRCULATION	VCRLC008
	F=.5*AR*(CHD**2)	VCRLC009
2	FORMAT(' FOR CIRCULATION USE:',F10.5,'*UINF*LIFT COEFFICIENT')	VCRLC010
	WRITE(IW,2) F	VCRLC011
	HC=CHD/FLOAT(NC)	VCRLC012
	HS=(CHD*AR/FLOAT(NS))	VCRLC013
	HS2=HS/2.	VCRLC014
	NP=NC+1	VCRLC015
	NS1=2*NS-1	VCRLC016
	CALL LOAD(SPL,CHL,NC,NS)	VCRLC017
	FAC=1./FLOAT(NC)	VCRLC018
	DO 10 I=1,NC	VCRLC019
10	CHL(I)=CHL(I)*FAC	VCRLC020
	FAC=AR/FLOAT(NS)	VCRLC021
	DO 20 I=1,NS	VCRLC022
20	SPL(I)=SPL(I)*FAC	VCRLC023
	DO 200 L=7,19,6	VCRLC024
	Y=HS*(L-1)	VCRLC025
	DO 100 M=1,NP	VCRLC026
	DW=C.0	VCRLC027
	X=(CHD/FLOAT(NC))*(M-1)	VCRLC028
	K=-1	VCRLC029
	KOAC=NS+1	VCRLC030
	B=1.	VCRLC031
	DO 50 IY=1,NS1	VCRLC032
	KOAC=KOAC+K	VCRLC033
	IF(KOAC.EQ.1) K=1	VCRLC034
	YC=-FS*NS+HS*IY	VCRLC035
	Y1=YC+FS2	VCRLC036

```
Y2=YC-HS2
DO 50 IX=1,NC
X1=HC*(IX-.5)
50 DW=DW+SPL(KCAD)*CHL(IX)*HORVOR(X,Y,X1,Y1,Y2)*B
100 W(M)=DW
WRITE(IW,3) (W(M),M=1,NP)
200 CONTINUE
3 FORMAT(' ',10E11.3)
STOP
END
```

```
VCRLC037
VCRLC038
VCRLC039
VCRLC040
VCRLC041
VCRLC042
VCRLC043
VCRLC044
VCRLC045
VCRLC046
```

```

C      FUNCTION HORVCR(X,Y,X1,Y1,Y2)
          FINITE HORSESHOE VORTEX DOWNWASH
DX=X1-X
DY1=Y1-Y
DY2=Y2-Y
DEN1=SQRT(DX**2+DY1**2)
DEN2=SQRT(DX**2+DY2**2)
HORVCR=(1./DY2)*(1.+DX/DEN2)-(1./DY1)*(1.+DX/DEN1)+(1./DX)*(DY2/DE
IN2-DY1/DEN1)
HORVOR=HORVCR/(4.*3.14159)
RETURN
END

```

```

HSVRC001
HSVRC002
HSVRC003
HSVRC004
HSVRC005
HSVRC006
HSVRC007
HSVRC008
HSVRC009
HSVRC010
HSVRC011
HSVRC012

```

	SUBROUTINE LOAD(SPL,CHL,NC,NS)	LC#10001
C	SPANWISE CUBIC CHORDWISE ELLIPTICAL	LC#10002
	DIMENSION SPL(30),CHL(10)	LC#10003
	HC=1./FLOAT(NC)	LC#10004
	AR=FLOAT(NS)/FLOAT(NC)	LC#10005
	HS=AR/FLOAT(NS)	LC#10006
	DO 100 I=1,NC	LC#10007
	X=HC*(I-.5)	LC#10008
100	CHL(I)=8.*SQRT(X-X**2)/3.14159	LC#10009
	DO 200 I=1,NS	LC#10010
	Y=FLOAT(I-1)*HS	LC#10011
200	SPL(I)=12.*(Y**2)*(AR-Y)	LC#10012
	RETURN	LC#10013
	END	LC#10014

	SUBROUTINE LOAD(SPL,CHL,NC,NS)	LC#20001
C	FOR ELLIPTICAL SPANWISE AND ELLIPTICAL CHORDWISE	LC#20002
	DIMENSION SPL(30),CHL(10)	LC#20003
	HC=1./FLOAT(NC)	LC#20004
	AR=FLOAT(NS)/FLCAT(NC)	LC#20005
	HS=AR/FLOAT(NS)	LC#20006
	DO 100 I=1,NC	LC#20007
	X=HC*(I-.5)	LC#20008
100	CHL(I)=8.*SQRT(X-X**2)/3.14159	LC#20009
	DO 200 I=1,NS	LC#20010
	Y=FLCAT(I-1)*HS	LC#20011
200	SPL(I)=4.*SQRT(AR**2-Y**2)/(3.14159*(AR**2))	LC#20012
	RETURN	LC#20013
	END	LC#20014

Appendix J

LIST OF COMPUTER PROGRAMS USED TO EVALUATE
THE DOWNWASH OF A POINT HORSESHOE VORTEX SINGULARITY

```

C      POINT HORSESHOE VORTEX: FREE SURFACE EFFECTS
C      PROGRAM ONE MODIFIED
COMMON CTH,CPH,STH,C2,CX,Y,F
COMMON THD,SPH,ER
DIMENSION DUM(1000),XN(20),YN(20)
DATA IR,IW/5,6/
DATA PI/3.14159/
4     FORMAT(3F6.3,2X,4E15.7)
5     FORMAT(' RESULTS ABOVE * SQRT Y: CAUCHY',E14.6,1X,'RESIDUE',E14.6,
11X,'UPSTREAM',E14.6,1X,'DOWNSTREAM',E14.6,////)
7     FORMAT(1H ,4E20.6,I10)
9     FORMAT(1H0,9HABS(X-X0),1X,F10.5,10X,11HCAUCHY PART,4X,E16.6,10X,17
1HDOWNWASH UPSTREAM,4X,E16.6)
10    FORMAT(1H ,4HY+YC,6X,F10.5,10X,12HRESIDUE PART,3X,E16.6,10X,19HCOW
1NWASH DOWNSTREAM,2X,E16.6,////)
14    FORMAT(2I5,2F10.5)
15    FORMAT(I10,2E20.6)
11    FORMAT(8F10.5)
20    FORMAT(1H ,53HTWICE INFINITE FLUID REVERSED IMAGE DOWNWASH UPSTREA
1M,3X,E15.6,3X,10HDOWNSTREAM,3X,E15.6)
13    READ(IR,14) NX,NY,F,ER
      IF(NX.LE.0) GOTO 4000
      WRITE(IW,14)NX,NY,F,ER
      READ(IR,11) (XN(I),I=1,NX)
      READ(IR,11) (YN(I),I=1,NY)
      DO 20000 IYY=1,NY
      DO 20000 IXX=1,NX
      DX=XN(IXX)
      Y=YN(IYY)
      PANS=0.0
      NI=10
      IB=2
      IE=10
      IS=1
      DUM(1)=0.0
50    NP=NI+1

```

```

KRNL0001
KRNL0002
KRNL0003
KRNL0004
KRNL0005
KRNL0006
KRNL0007
KRNL0008
KRNL0009
KRNL0010
KRNL0011
KRNL0012
KRNL0013
KRNL0014
KRNL0015
KRNL0016
KRNL0017
KRNL0018
KRNL0019
KRNL0020
KRNL0021
KRNL0022
KRNL0023
KRNL0024
KRNL0025
KRNL0026
KRNL0027
KRNL0028
KRNL0029
KRNL0030
KRNL0031
KRNL0032
KRNL0033
KRNL0034
KRNL0035
KRNL0036

```

	H=1./FLOAT(NI)	KRNLC037
	DO 100 I=IB,IE,IS	KRNLC038
	D=H*(I-1)	KRNLC039
	TH=PI*(1.-D**2)/2.	KRNLC040
	THD=90.*TH/1.5708	KRNLC041
	CALL WNINT(TH,ANS)	KRNLC042
	DUM(I)=ANS*C*PI	KRNLC043
100	CONTINUE	KRNLC044
	DUM(NP)=0.0	KRNLC045
	CALL SIMR(NI,H,DUM,ANS)	KRNLC046
	IF (ABS(ANS).LE.1.E-50) GOTO 200	KRNLC047
	TEST=ABS((ANS-PANS)/ANS)	KRNLC048
	IF (TEST.LE.ER) GOTO 202	KRNLC049
	PANS=ANS	KRNLC050
	NI=NI*2	KRNLC051
	IF(NI.GE.1000) GOTO 200	KRNLC052
	CALL SPRD(DUM,NP)	KRNLC053
	IB=2	KRNLC054
	IE=NI	KRNLC055
	IS=2	KRNLC056
	GOTO 50	KRNLC057
200	WRITE(IW,15) NI,TEST,ANS	KRNLC058
202	CONTINUE	KRNLC059
	CINT=ANS	KRNLC060
C	RESIDUE PART OF KERNEL	KRNLC061
	SUM=0.0	KRNLC062
	N=-1	KRNLC063
	T1=0.0	KRNLC064
2800	N=N+1	KRNLC065
	NS=4	KRNLC066
	T2=F*Y*((3.14159*(N+.5)/(F*DX))**2-1.)	KRNLC067
	IF (T2.LE.0.0) GOTO 2800	KRNLC068
	IF (T2.GE.170.) T2=170.	KRNLC069
	PANS=0.0	KRNLC070
2900	DT=(T2-T1)/FLOAT(NS)	KRNLC071
	NS2=NS+1	KRNLC072

	DO 3000 I=1,NS2	KRNLC073
	J=I-1	KRNLC074
	Q=J*DT+T1	KRNLC075
3000	DUM(I)=RFUN(Q)*EXP(-Q)	KRNLC076
	CALL SIMR(NS,DT,DUM,ANS)	KRNLC077
	IF (ABS(ANS).LT.1.E-50) GOTO 3500	KRNLC078
	TEST=ABS((ANS-PANS)/ANS)	KRNLC079
	IF (TEST.LT.ER) GOTO 3500	KRNLC080
	IF (ABS(ANS).LT.ABS(SUM)/ER) GOTO 3500	KRNLC081
	IF (NS.GT.256) GOTO 3500	KRNLC082
	PANS=ANS	KRNLC083
	NS=NS*2	KRNLC084
	GOTO 2900	KRNLC085
3500	CONTINUE	KRNLC086
	SUM=SUM+ANS	KRNLC087
	IF (T2.GE.170.) GOTO 3700	KRNLC088
	IF (ABS(SUM).LE.1.E-50) GOTO 3700	KRNLC089
	TEST=ABS(ANS/SUM)	KRNLC090
	IF (TEST.LT.ER) GOTO 3800	KRNLC091
	T1=T2	KRNLC092
	GOTO 2800	KRNLC093
3700	WRITE(IW,7) T1,T2,ANS,TEST,NS	KRNLC094
3800	SUM=SUM*(-EXP(-F*Y)*4*F/Y)	KRNLC095
	UPST=CINT	KRNLC096
	DOWN=SUM-CINT	KRNLC097
	WRITE(IW,9) DX,CINT,UPST	KRNLC098
	WRITE(IW,10) Y,SUM,DOWN	KRNLC099
	WRITE(7,4) DX,Y,F,SUM,CINT,UPST,DOWN	KRNLC100
	HV1=1./(Y**2)	KRNLC101
	HV2=-DX/((Y**2)*SQRT(DX**2+Y**2))	KRNLC102
	HVUP=-2.*(HV1+HV2)	KRNLC103
	HVDN=-2.*(HV1-HV2)	KRNLC104
	WRITE(IW,20) HVUP,HVDN	KRNLC105
	FY=SQRT(Y)	KRNLC106
	CINT=CINT*FY	KRNLC107
	UPST=UPST*FY	KRNLC108

```
SUM=SUM*FY
DOWN=DCWN*FY
WRITE(IW,5) CINT,SUM,UPST,DCWN
20000 CONTINUE
      GOTO 13
4000  STOP
      END
```

```
KRNLO109
KRNLO110
KRNLO111
KRNLO112
KRNLO113
KRNLO114
KRNLO115
```

	SUBROUTINE WNINT(TH,ANS)	WVNIC001
C	INTEGRAL OVER WAVE NUMBERS	WVNIC002
	COMMON CTH,CPH,STH,C2,DX,Y,F	WVNIC003
	COMMON THD,SPH,ER	WVNIC004
	DIMENSION V(7),w(7)	WVNIC005
	DIMENSION DUM(1000)	WVNIC006
	DATA V/.19304,1.0266,2.56788,4.90035,8.18215,12.73418,19.39573/	WVNIC007
	DATA W/4.09319E-01,4.21831E-01,1.47126E-01,2.06335E-02,1.07401E-03	WVNIC008
	1,1.58655E-05,3.17032E-08/	WVNIC009
1	FORMAT(I5,6E17.6)	WVNIC010
	IR=5	WVNIC011
	IW=6	WVNIC012
	CTH=COS(TH)	WVNIC013
	STH=SIN(TH)	WVNIC014
	A1=0.0	WVNIC015
	A2=0.0	WVNIC016
	A4=0.0	WVNIC017
	A3=0.0	WVNIC018
	DEN=SQRT(Y**2+(DX*CTH)**2)	WVNIC019
	CPH=Y/DEN	WVNIC020
	SPH=-DX*CTH/DEN	WVNIC021
	DS=DX*CTH/Y	WVNIC022
	PP=DS**2	WVNIC023
	DS=1.732*DS	WVNIC024
	IF (PP.GT.3.0) GOTO 411	WVNIC025
	SZC=0.5*(3.-PP)	WVNIC026
	CP=1.	WVNIC027
	IF (ABS(SZC-1.).GT.DS) GOTO 70	WVNIC028
	CP=SZC	WVNIC029
	DS=2.*DS	WVNIC030
C	INTEGRATE REGION NEAR THE NUMERICAL SINGULARITY	WVNIC031
70	PANS=0.0	WVNIC032
	TEST=0.0	WVNIC033
	IB=1	WVNIC034
	IE=3	WVNIC035
	IS=1	WVNIC036

	IF(DS.GT.CP) DS=CP	WVNI0037
	NI=2	WVNI0038
90	NP=NI+1	WVNI0039
	H=2.*DS/FLOAT(NI)	WVNI0040
	DO 100 I=IB,IE,IS	WVNI0041
	S=CP-DS+(I-1)*H	WVNI0042
100	DUM(I)=FUNS(S)	WVNI0043
	CALL SIMR(NI,H,DUM,ANS)	WVNI0044
	IF(ABS(ANS).LE.1.E-50) GOTO 110	WVNI0045
	TEST=ABS((ANS-PANS)/ANS)	WVNI0046
	IF (TEST.LE.ER) GOTO 110	WVNI0047
	IF (NI.GT.256) GOTO 105	WVNI0048
	CALL SPRD(DUM,NP)	WVNI0049
	NI=NI*2	WVNI0050
	IB=2	WVNI0051
	IE=NI	WVNI0052
	IS=2	WVNI0053
	PANS=ANS	WVNI0054
	GOTO 90	WVNI0055
105	WRITE(IW,1) NI,DS,H,THD,ANS,TEST	WVNI0056
110	A1=ANS	WVNI0057
C	INTEGRATE REGION ZERO TO PEAK REGION	WVNI0058
	PANS=0.0	WVNI0059
	IF(DS.GE.CP) GOTO 211	WVNI0060
	IB=2	WVNI0061
	IE=3	WVNI0062
	IS=1	WVNI0063
	DUM(1)=0.0	WVNI0064
	TEST=0.0	WVNI0065
	NI=2	WVNI0066
190	NP=NI+1	WVNI0067
	H=(CP-DS)/FLOAT(NI)	WVNI0068
	DO 200 I=IB,IE,IS	WVNI0069
	S=(I-1)*H	WVNI0070
200	DUM(I)=FUNS(S)	WVNI0071
	CALL SIMR(NI,H,DUM,ANS)	WVNI0072

	IF (ABS(ANS).LE.1.E-50) GOTO 210	WVNIC073
	TEST=ABS((ANS-PANS)/ANS)	WVNIC074
	IF (TEST.LE.ER) GOTO 210	WVNIC075
	IF (NI.GT.256) GOTO 205	WVNIC076
	CALL SPRD(DUM,NP)	WVNIC077
	NI=NI*2	WVNIC078
	IB=2	WVNIC079
	IE=NI	WVNIC080
	IS=2	WVNIC081
	PANS=ANS	WVNIC082
	GOTO 190	WVNIC083
205	WRITE(IW,1) NI,DS,H,A1,THD,ANS,TEST	WVNIC084
210	A2=ANS	WVNIC085
211	CONTINUE	WVNIC086
C	INTEGRATE REGION JUST BEYOND SINGULAR POINT	WVNIC087
	IF(CP+DS.LT.SZC) GOTO 385	WVNIC088
	SUL=CP+DS	WVNIC089
	GOTO 411	WVNIC090
385	SUL=2.*SZC-CP-DS	WVNIC091
	PANS=0.0	WVNIC092
	IB=1	WVNIC093
	IE=3	WVNIC094
	IS=1	WVNIC095
	TEST=0.0	WVNIC096
	NI=2	WVNIC097
390	NP=NI+1	WVNIC098
	H=2.*(SZC-CP-DS)/FLOAT(NI)	WVNIC099
	DO 400 I=IB,IE,IS	WVNIC100
	S=CP+DS+H*(I-1)	WVNI0101
400	DUM(I)=FUNS(S)	WVNI0102
	CALL SIMR(NI,H,DUM,ANS)	WVNIC103
	IF (ABS(ANS).LE.1.E-50) GOTO 410	WVNI0104
	TEST=ABS((ANS-PANS)/ANS)	WVNI0105
	IF (TEST.LE.ER) GOTO 410	WVNI0106
	IF (NI.GT.256) GOTO 405	WVNI0107
	CALL SPRD(DUM,NP)	WVNI0108

	NI=NI*2	WVNI0109
	IB=2	WVNI0110
	IE=NI	WVNI0111
	IS=2	WVNI0112
	PANS=ANS	WVNI0113
	GOTO 390	WVNI0114
405	WRITE(IW,1) NI,SUL,H,A1,THD,ANS,TEST	WVNI0115
410	A4=ANS	WVNI0116
411	CONTINUE	WVNI0117
C	LAGUERRE POLYNOMIAL INTERPOLATION QUADRATURE TO INFINITY	WVNI0118
	SS=SUL	WVNI0119
	DC 300 I=1,7	WVNI0120
	S=SS+V(I)	WVNI0121
	T1=FUNS(S)	WVNI0122
	BF=1.	WVNI0123
	IF(T1.LT.0.0) BF=-1.	WVNI0124
	IF(T1.EQ.0.0) GOTO 300	WVNI0125
	T1=ABS(T1)	WVNI0126
	E1=ALOG(T1)	WVNI0127
	E2=V(I)	WVNI0128
	E3=ALOG(W(I))	WVNI0129
	E=E1+E2+E3	WVNI0130
	IF (ABS(E).GT.170.) GOTO 300	WVNI0131
	A3=A3+BF*EXP(E)	WVNI0132
300	CONTINUE	WVNI0133
	ANS=A1+A2+A3+A4	WVNI0134
	RETURN	WVNI0135
	END	WVNI0136

```

FUNCTION FUNS(S)
COMMON CTH,CPH,STH,C2,DX,Y,F
COMMON THD,SPH,ER
IF (S.LE.0.0) GOTO 20
PP=(DX*CTH/Y)**2
T1=(4./3.14159)*(F**2)
T2=STH**2
T3=(DX/Y)*(S**2)
T4=2.*S-3.+PP
T5=-F*Y*S/(CTH**2)
T6=(1.+PP)**2
T7=S**2-2.*S+1.+PP
T8=CTH**4
IF (T8.LE.0.0) GOTO 20
TEST=T5-ALOG(T8)
IF (ABS(TEST).GT.160.) GOTO 20
FUNS=(T1*T2*T3*T4/(T6*T7))*EXP(TEST)
RETURN
FUNS=0.0
RETURN
END

```

```

FUNSC001
FUNSC002
FUNSC003
FUNSC004
FUNSC005
FUNSC006
FUNSC007
FUNSC008
FUNSC009
FUNSC010
FUNSC011
FUNSC012
FUNSC013
FUNSC014
FUNSC015
FUNSC016
FUNSC017
FUNSC018
FUNSC019
FUNSC020
FUNSC021

```

20

```
FUNCTION RFUN(Q)
COMMON CTH,CPH,STH,C2,DX,Y,F
COMMON THD,SPH,ER
X1=Q/(F*Y)
RFUN=SQRT(X1*(X1+1))*CCS(F*DX*SQRT(X1+1))
RETURN
END
```

```
RFUNC001
RFUNC002
RFUNC003
RFUNC004
RFUNC005
RFUNC006
RFUNC007
```

```
SUBROUTINE SIMR(NI,H,FUNC,ANS)
DIMENSION FUNC(1000)
K=NI+1
ANS=FUNC(1)+FUNC(K)
10 DO 10 J=2,NI,2
ANS=ANS+4*FUNC(J)
IF(NI.EQ.2)GOTO 30
K=NI-1
20 DO 20 J=3,K,2
ANS=ANS+2*FUNC(J)
30 ANS=ANS*H/3.
RETURN
END
```

```
SIMR001
SIMR002
SIMR003
SIMR004
SIMR005
SIMR006
SIMR007
SIMR008
SIMR009
SIMR010
SIMR011
SIMR012
SIMR013
```

BIOGRAPHICAL NOTE

Edward C. Kern, Jr. was born on June 1, 1945 and attended the Lawrenceville School in Lawrenceville, New Jersey. He received the degree Artium Baccalaureus from Dartmouth College in 1967 and the degree Bachelor of Engineering from the Thayer School of Engineering at Dartmouth College in 1968. He then entered the Graduate School at Massachusetts Institute of Technology and received the S.M. and Ocean Engineer's degrees in 1971. While at Massachusetts Institute of Technology he has held appointments as teaching assistant, research assistant and DSR engineer. He is a member of Sigma Xi.